**MASARYK UNIVERSITY**

**FACULTY OF SCIENCE**

**DEPARTMENT OF BIOCHEMISTRY**

# <u>Elicitins impact on the proteome of tobacco</u>

**Master Thesis**

Brno 2010

Ladislav Dokládal

**Název česky:** Vliv elicitinů na změny proteomu tabáku

**Abstrakt česky:**

Kryptogein je proteinový elicitor sekretovaný oomycetou *Phytophthora cryptogea*. V rostlinách tabáku je schopen indukovat rezistenci vůči *P. parasitica*. Na základě dříve provedeného počítačového modelování byly připraveny mutantní formy kryptogeinu s alterovanou schopností vázat steroly, fosfolipidy či obojí, přičemž schopnost vazby sterolů a transferu fosfolipidů jsme ověřili i experimentálně. Úroveň indukce syntézy reaktivních forem kyslíku (ROS) v suspenzi tabákových buněk a proteomických změn v mezibuněčné tekutině listů tabáku vyvolaných těmito mutantními elicitiny nebyla úměrná jejich schopnostem vázat či transportovat steroly a fosfolipidy. Změny v intercelulárním proteomu však odpovídaly úrovním transkripce obranných genů a rezistence vůči *P. parasitica*, přičemž nebyly predikovány významné změny ve struktuře připravených mutantních proteinů. Naše výsledky nejsou ve shodě s dřívějšími předpoklady a naznačují, že sterol-vazebné schopnosti kryptogeinu a jeho mutantů a s nimi asociované změny konformace ω-smyčky nemusí být zásadními faktory řídícími produkci ROS či indukci rezistence. Výsledky nicméně podporují význam ω-smyčky při interakci elicitinu s vysoce afinitním vazebným místem na cytoplasmatické membráně buněk tabáku.

**Klíčová slova:**

elicitor, elicitin, kryptogein, PR proteiny, fytoalexin kapsidiol, hypersensitivní odpověď, místně specifická mutagenese, 2-D electroforesa, *Pichia pastoris*

**Title in English:** Elicitins impact on the proteome of tobacco

**Abstract in English:**

Cryptogein is a proteinaceous elicitor secreted by an oomycete *Phytophthora cryptogea* that can induce resistance to *P. parasitica* in tobacco plants. On the basis of previous computer modeling, a series of cryptogein mutants was prepared with altered abilities to bind sterols, phospholipids or both. The sterol binding and phospholipid transfer activities corresponded to expectations based on the structural data reported previously. Induction of synthesis of reactive oxygen species (ROS) in tobacco cells suspension and proteomic analysis of intercellular fluid changes in tobacco leaves triggered by these mutant elicitins were not proportional to their ability to bind or transfer sterols and phospholipids. However, changes in the intercellular proteome corresponded to transcription levels of defense genes and resistance to *P. parasitica* and structure-prediction of mutants did not reveal any significant changes in protein structure. These results suggest, contrary to previous proposals, that the sterol-binding ability of cryptogein and its mutants, and the associated conformational change in the ω-loop, might not be principal factors in either ROS production or resistance induction. Nevertheless results support importance of ω-loop for interaction of the elicitin with the high affinity binding site on the plasma membrane of tobacco cells.

*Declaration*

*I hereby declare and confirm that this thesis is entirely the result of my own work except where otherwise indicated.*

*Brno, 16.4.2010*                                                                                   *Ladislav Dokládal*

**Content**

| | |
|---|---|
| ABA | abscisic acid |
| AtMPK4 | *Arabidopsis thaliana* MAPK4 |
| AOX | alternative oxidase |
| Bax | B-cell leukemia lymphoma 2 – associated X protein |
| bZIP | basic leucine-zipper 2 |
| cAPDR | cyclic ADP ribose |
| CaM | calmodulin |
| CBP20 | chitin-binding protein 20 |
| CDPK | $Ca^{2+}$-dependent protein kinase |
| CHAPS | 3-[(3-cholamidopropyl)dimethylammonio]-1-propanesulfonate |
| Chi-V | class V chitinase |
| CPA | *cis*-parinaric acid |
| DAG | diacylglycerol |
| DHE | dehydroergosterol |
| DTT | 1,4-dithio-DL-threitol |
| ERF1 | ethylene response factor 1 |
| EDR1 | enhanced disease resistance 1 |
| ET | ethylene |
| HR | hypersensitive response |
| IEF | isoelectric focusing |
| $IP_3$ | inositol-1,4,5-trisphosphate |
| IPG | immobilized pH gradient |
| IRP-1 | iron regulatory protein-1 |
| JA | jasmonate |
| JIN1 | jasmonate insensitive1 |
| LOX2 | lipoxygenase 2 |
| MAPK | mitogen-activated protein kinase |
| MAPKK | MAPK kinase |
| MAPKKK | MAPKK kinase |
| MeJA | methyl jasmonate |
| NBD-PC | nitrobenzoxadiazole-labelled phosphatidylcholine |
| NPR1 | nonexpressor of PR1 |

| | |
|---|---|
| NtChitIV | *Nicotiana tabacum* class IV chitinase |
| NtPRp27 | *Nicotiana tabacum* PR protein 27 |
| PA | phosphatidic acid |
| PAL | phenylalanine ammonia lyase |
| PC | phosphatidylcholine |
| PCD | programmed cell death |
| PI | phosphatidylinositol |
| PIP | phosphatidylinositol-4-phosphate |
| $PIP_2$ | phosphatidylinositol-(4,5)-bisphosphate |
| PMSF | phenylmethanesulfonyl fluoride |
| PLA1 | phospholipase A1 |
| PLA2 | phospholipase A2 |
| PLC | phospholipase C |
| PLD | phospholipase D |
| PR | pathogenesis-related |
| PS | phosphatidylserine |
| ROS | reactive oxygen species |
| SA | salicylate |
| SABP | SA-binding protein |
| SAR | systemic acquired resistance |
| SDS | sodium dodecyl sulfate |
| SDS-PAGE | SDS-polyacrylamide gel electrophoresis |
| TMV | tobacco mosaic virus |
| tpoxN1 | tobacco peroxidase N1 |
| SIPK | SA-induced protein kinase |
| WIPK | wounding-induced protein kinase |
| wt | wild type |

## *Introduction*

Among the causal agents of infectious plant diseases, phytopathogenic fungi and oomycetes play the dominant role (*1*). Approximately 10 percent of all fungi and oomycetes have acquired the ability to colonize plants or to cause disease (*2*). Infection of crop plants has repeatedly resulted in catastrophic harvest failures that have caused major economic and social problems in the affected countries (*1*). The potential for serious crop epidemics still persists today, as evidenced by recent outbreaks of diseases caused by rust, mildew, or *Phytophthora* species. In addition to causing food shortages, fungal infection of plants can directly affect the health of humans and livestock through poisoning by toxins. As use of fungicides causes environmental problems, new approaches have to be found.

Over the past two decades, a number of different approaches have been considered by plant pathologists towards enhancing plant disease resistance (*3*). Among these, the use of non-specific resistance elicitors, as part of an integrated disease control strategy, offers exciting opportunities although it is clear that unequivocal answers to key questions including the stability and persistence of induced host response, the efficiency of such molecules under commercial conditions, and their suitability in an integrated crop protection system need to be answered before elicitors can be considered as powerful crop protectants.

Furthermore, genetic engineering has led to the development of crop plants with enhanced resistance to fungal pathogens (*1*). However, genetic engineering for disease resistance is still in its infancy. Thus, intensified research uncovering the molecular basis of both fungal pathogenicity and plant disease resistance is required to better protect plants against microbial invasion. Because manipulation of signal-transduction pathways is believed to be one of the ways to engineer crop plants with enhanced disease resistance, research in this area has gained enormous momentum in recent years. Better understanding of defense signaling will provide new tools for engineering fungal disease resistance in plants.

*Theoretical part*

## 1. <u>Perception of pathogen signals in plants</u>

Molecular communications between plant and pathogen start almost immediately after the pathogen makes contact with the plant surface (*4*). On perception of the plant signals, pathogen prepares to invade the host tissues by using its various toxic mechanisms. On the other hand, plants perceive the pathogen signals and prepare to defend themselves by rigidification of cell wall, producing several antimicrobial compounds to ward off the pathogens. According to the virulence of plant pathogens, two types of plant-pathogen interactions can be observed: compatible and incompatible. In compatible interactions the virulent pathogen can spread in the susceptible plant (*5*). On the other hand, in incompatible interactions the plant is resistant and can successfully prevent the pathogen spreading. The successful defense is based on the early recognition of avirulent strains of plant pathogens and the fast activation of defense.

### 1.1 Elicitors

The term elicitor was first used to describe the molecules that are capable of eliciting the production of phytoalexins (*4*). Today, it is commonly used for compounds eliciting any type of plant defense.

Elicitors can be divided into two groups (*4*):

1) exogenous (microbial) elicitors – substances of pathogen origin:
    a. general elicitors, able to trigger defense responses in both host and non-host plants,
    b. race-specific elicitors, inducing defense responses leading to disease resistance only in specific host cultivars,

2) endogenous (host plant) elicitors – compounds that are released from plants due to pathogen's action.

Elicitors have different chemical structure and can belong to oligosaccharides, proteins, peptides, glycoproteins, or lipids (*4*). According to the so-called gene-for-gene hypothesis, a race specific elicitor encoded by or produced by the action of an avirulence (*avr*) gene present in a particular race of pathogen elicits resistance only in a host plant variety carrying the corresponding resistance (*R*) gene.
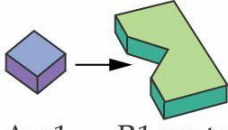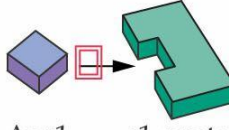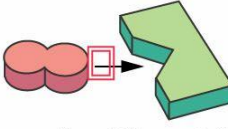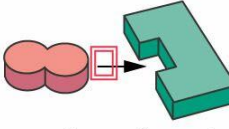
**Figure 1**: Gene-for-gene model. For resistance (incompatibility) to occur, complementary pairs of dominant genes, one in the host and one in the pathogen, are required. An alteration or loss of the plant resistance gene (*R* changing to *r)* or of the pathogen avirulence gene (*Avr* changing to *avr*) leads to disease (compatibility). (*6*)

## 1.2    Elicitins

The term elicitins describes a family of structurally related proteins secreted by several *Phytophthora* and *Pythium* spp. (*4*). All elicitins share a conserved elicitin domain of 98 amino acids that are interconnected by three disulfide bridges (*7*).

On the basis of their primary structure, elicitins can be grouped into five classes (*4*):

a.  class I-A (α-elicitins) – 10 kDa proteins containing only the elicitin domain and having an acidic pI,

b.  class I-B (β-elicitins) – 10 kDa proteins containing only the elicitin domain as well, but having a basic pI,

c.  class II – highly acidic elicitins with a short (5-6 amino acids), hydrophilic C-terminal tail,

d.  class III – elicitins with a long (65-101 amino acids) C-terminal domain rich in serine, threonine, alanine, and proline residues, suggesting potential O-glycosylation,

e.  Py class – elicitins from *Pythium* spp., structurally related to the class I elicitins.

The class I-A and the class I-B elicitins are holo-proteins lacking side chain modification (*4*). The β-elicitins generally induce a greater necrotic effect than the α-elicitins due to the presence of polar amino acids at necrotic sites located on the protein surface (*7*). Elicitins did not exhibit

any protease, β-glucanase, or phospholipase activity, and no other enzymatic activity has been reported so far (*8*).

## 2.     <u>**Transduction of pathogen signals in plants**</u>

The signal transduction networks linking receptor-mediated perception of pathogens and defense reactions employ second messengers that are conserved among most eukaryotes (*1*). Second messengers of mammalian innate immunity, such as $Ca^{2+}$, ROS (reactive oxygen species), NO and mitogen-activated protein kinase (MAPK) cascades, are also involved in defense signaling in plants. Furthermore, phospholipid-signaling system, anion channels, cytoplasmic acidification, salicylic acid (SA)-signaling system, jasmonate-signaling pathway, ethylene (ET)-dependent signaling pathway, and abscisic acid (ABA) signaling play an important role in transduction of pathogen signals in plants.

### 2.1     **Calcium ion as second messenger**

$Ca^{2+}$ acts as an intacelullar second messenger, coupling extracellular stimuli to intracellular and whole-plant responses (*9*). Elicitor treatment induces rapid $Ca^{2+}$ influx into cytoplasm of plant cells (*10*). Massive influx of $Ca^{2+}$ in tobacco-cultured cells was observed within 15-30 min after treatment with an elicitin cryptogein. Elicitation of defense response was more effective in the presence of $Ca^{2+}$ in plants (*4*).

$Ca^{2+}$ concentration increases in plant cells by two ways: influx of $Ca^{2+}$ across the plasma membrane and release of $Ca^{2+}$ from internal stores (*4*). $Ca^{2+}$ permeation through the plant plasma membrane may occur due to the activation of $Ca^{2+}$-permeable channels either at hyperpolarized or at depolarized membrane potentials. It was suggested that the activation of the channel by fungal elicitors is modulated by a heterotrimeric G-protein-dependent phosphorylation of the channel protein.

Pathogen signals may trigger an oscillation in the cytosolic free $Ca^{2+}$ concentration which is then perceived by various intracellular sensors or binding proteins to regulate a series of signaling cascades (*4*). $Ca^{2+}$ sensors can be classified into sensor responders and sensor relay (*11*). On binding with $Ca^{2+}$, sensor responders, e.g. $Ca^{2+}$-dependent protein kinases (CDPKs), change their conformation and modulate their own activity or function through intramolecular interactions. Sensor relay, like calmodulin (CaM), communicates the changed conformation to interacting partners such as protein kinases, resulting in a change in their activity.

## 2.2 Phosphorylation of proteins in signal transduction

Posttranslational protein phosphorylation is a general mechanism in the transduction of signals originating from pathogens (*4*). Changes in the level of phosphorylation of plant cellular proteins have been observed upon elicitor treatments of a variety of cell cultures. Activation of protein kinases and inhibition of protein phosphatases may result in increased phosphorylation of proteins that trigger the induction of host plant defense responses.

The phosphorylation of membrane proteins is dependent on $Ca^{2+}$ in many cases. $Ca^{2+}$-dependent protein kinase (CDPK), $Ca^{2+}$-/CaM-dependent protein kinase, protein kinase C, and $Ca^{2+}$-modulated phosphatases play an important role in protein phosphorylation (*10*). The targets of plant CDPKs remain to be identified but may be related to animal protein kinase C, which is involved in activation of the NADPH oxidase of mammalian neutrophils (*1*). Besides CDPK, other protein kinases may also be involved in elicitor-induced protein phosphorylation. For example, activation of a 40 kDa protein kinase was dependent on $NO_3^-$ efflux induced by the elicitor treatment (*12*).

MAPKs have been shown to be also involved in plant defense reactions (*4*). MAPK cascades form an important component in the signaling machinery that transduces extracellular signals into a wide range of intracellular responses, and are believed to represent a central point of cross-talk in stress signaling in plants. Activation of MAPKs by elicitors from different plant pathogens in various plant species has been reported. The MAPK cascade involves three functionally linked protein kinases, such as a MAP kinase kinase kinase (MAPKKK), a MAP kinase kinase (MAPKK), and a MAP kinase (MAPK). In response to extracellular signals, an MAPKKK activates an MAPKK via phosphorylation of serine (S) and serine/threonine residues within the SXXXS/T motif, where X denotes any amino acid. An MAPKK, which is a dual-specificity protein kinase, then activates an MAPK by phosphorylating specific effector proteins, which leads to activation of cellular responses. MAPK activation is located downstream of the elicitor-stimulated $Ca^{2+}$ influx and appears not to be necessary for the oxidative burst (*1*). Several types of MAPKs have been recognized (*4*). Rapid activation of SA-induced protein kinase (SIPK) and transient activation of wounding-induced protein kinase (WIPK) by cryptogein elicitor in tobacco have been reported (*13*), as well as a MAPK mediating ET-signaling (*4*). Remarkably, some MAPK cascades were found to be negative regulators of plant defense (*1*). *Arabidopsis* mutants carrying a transposon insertion in the *AtMPK4* gene had an extreme dwarf phenotype and exhibited elevated SA levels, constitutive *PR* (*pathogenesis related*) gene expression, and increased resistance against virulent pathogens.

## 2.3    Phospholipid signaling

Several phospholipids commonly found in plant membranes play important roles in signal transduction (*4*). Phosphatidylcholine (PC) and phosphatidylinositol (PI) are the major groups of membrane lipids. The inositol headgroup can be reversibly phosphorylated at various positions by the combined action of various kinases and phosphatases, producing different phosphoinositides, such as phosphatidylinositol, phosphatidylinositol-4-phosphate (PIP), and phosphatidylinositol-(4,5)-bisphosphate (PIP$_2$). Activities of PI kinase and PIP kinase were elevated *in vitro* by a fungal elicitor treatment. Also, several membrane-associated phospholipases are involved in releasing various other phospholipids, such as phospholipase A1 (PLA1), PLA2, PLC and PLD.

PLA1 and PLA2 catalyze the hydrolysis of a diacylglycerolphospholipid, producing a free fatty acid and a lysophospholipid. The fatty acids released by PLA2 are likely to act as second messengers in the transmission of systemin-triggered signaling, but may also activate octadecanoid-signaling pathway (*4*). An increase of PLA2 activity has been correlated with the perception of elicitors in several plant-pathogen systems and with the production of ROS.

PLC hydrolyzes PIP and PIP$_2$ and produces diacylglycerol (DAG) and inositol-1,4,5-trisphosphate (IP$_3$) stimulating Ca$^{2+}$ efflux (*4*). An increase of IP$_3$ in elicitor-treated pea has been reported. DAG activates protein kinase C and protein phosphorylation and stimulates synthesis of IP$_3$, which leads to further release of Ca$^{2+}$ from internal stores. DAG is rapidly phosphorylated to phosphatidic acid (PA) by DAG kinase. PA triggers production of superoxide anion and can be further metabolized by PA phosphorylase to form DAG. DAG and PA greatly enhance the elicitor-induced phytoalexin accumulation.

PLD, which is often the most abundant phospholipase in plants, hydrolyzes PC, producing PA and choline (*4*). Fungal elicitors increase PLD activity. Cellular activity of PLD is regulated by several messengers such as Ca$^{2+}$ and polyphosphoinositides, GTP-binding proteins, H$_2$O$_2$, pH changes, and membrane perturbation.

Another phospholipid detected in plants is sphingomyelin (ceramid phosphorylcholine). Sphingomyelinase is an important phospholipid-degrading enzyme and it generates ceramide and sphingosine (*14*). Ceramide activates MAPKs and triggers hypersensitive cell death and defense reactions in tomato. Sphingosine stimulates the production of IP$_3$. Sphingosine-1-phosphate has a second messenger activity and it is involved in the inositol-independent release of Ca$^{2+}$ from intracellular stores and in anion efflux stimulation. It also acts as a ligand for certain GTP-binding protein coupled receptors.
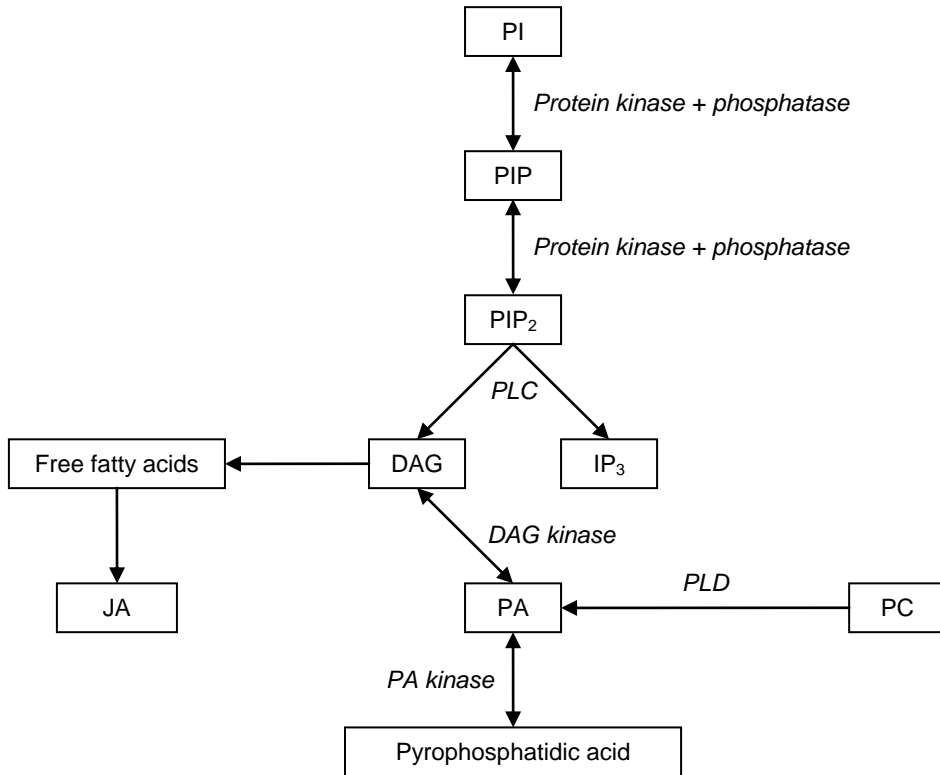
**Figure 2:** Pathway of biosynthesis of phospholipids (*4*). PC = phosphatidylcholine, PI = phosphatidylinositol, PIP = phosphatidylinositol-4-phosphate, $PIP_2$ = phosphatidylinositol-(4,5)-bisphosphate, DAG = diacylglycerol, $IP_3$ = inositol-1,4,5-trisphosphate, PA = phosphatidic acid, JA = jasmonate.

## 2.4 Anion channels, extracellular alkalinization, and cytoplasmic acidification in signal transduction

The elicitors-activated plasma membrane anion channels are one of the essential components of early signal transduction processes in plants (*4*). Anion channels may mediate $Cl^-$ and $NO_3^-$ efflux. $Cl^-$ efflux is one of the earliest events in elicitor-treated tobacco cells. Activation of $NO_3^-$ efflux depends on protein phosphorylation (*12*). Phosphatases negatively control the anion channel cascade, whereas protein kinases act as positive regulators in the chain of events leading to anion channel activity. $Ca^{2+}$ influx was found to be required for the initiation and maintenance of the anion channel in the cryptogein-treated cells. The link between $Ca^{2+}$ influx and anion efflux may involve a complex network of signals, including nucleotides, phosphorylation/dephosphorylation events, cytoplasmic free $Ca^{2+}$, voltage, and cytoplasmic pH. The anion channels blockers, such as niflumic acid, glibenclamide, and ethacrynic acid, reduced and delayed the hypersensitive cell death and the induction of several defense-related genes in tobacco plants. Oxidative burst and induction of a 40 kDa protein kinase are the downstream events of the anion channel-signaling system. Alkalinization of the extracellular medium may

occur if an efflux of anions resulting from channel activation provided substrate for a $H^+$/anion symporter at the plasma membrane.

Cytoplasmic acidification by biotic or abiotic stress is considered a plant-specific trigger for the synthesis of phytoalexins and other secondary metabolites (*15*). The simultaneous increase of external pH originates from an influx of protons into the challenged cells (*4*). It is due to the inhibition of the plasma membrane $H^+$-ATPase via reversible phosphorylation. Reversible changes of the phosphorylation state of the proton pump have been found to occur after exposure of tomato cells to a fungal pathogen.

## 2.5 Reactive oxygen species in signal transduction

The oxidative burst, which is a rapid and transient production of ROS, including $O_2^-$, $H_2O_2$, hydroxyl radical ($^\cdot OH$), and singlet oxygen ($^1O_2$), is the fastest active defense response induced by pathogens in the resistant interactions (*4*). The accumulation of ROS has been recognized as an early event of the plant defense responses.

The first reaction during the pathogen-induced oxidative burst is the one-electron reduction of molecular oxygen to form $O_2^-$ (*16*):

$$2O_2 + NADPH \rightarrow 2O_2^- + NADP^+ + H^+.$$
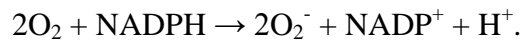
$O_2^-$ bears an unpaired electron and is routinely generated, in low concentrations, by the electron transport system (*4*). $O_2^-$ is also produced by the action of a number of enzymes, which participate in oxidation-reduction processes, such as NADPH oxidase, NADPH peroxidase, lipoxygenase, and xanthine oxidase.

$H_2O_2$ may be produced from $O_2^-$, which undergoes spontaneous dismutation, or through the action of superoxide dismutase (*16*):

$$2O_2^- + 2H^+ \rightarrow H_2O_2 + O_2.$$
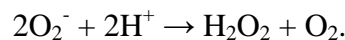
Plants may produce $H_2O_2$ via an NADPH oxidase system, peroxidases, xanthine oxidase, oxalate oxidase, urate oxidase, and glycollate oxidase (*4*). SA inhibits catalase, which can remove $H_2O_2$, and thus SA may increase the accumulation of $H_2O_2$ in plant cells.

$O_2^-$ reacts with $H_2O_2$ to produce hydroxyl radical (*17*):

$$O_2^- + H_2O_2 + H^+ \rightarrow H_2O + O_2 + {}^\cdot OH.$$
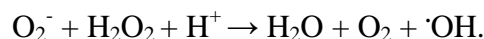
$O_2^-$ can also act as a reducing agent for transition metals such as $Fe^{3+}$ and $Cu^{2+}$ (*18*). These metals may be reduced even if they are complexed with proteins or low molecular weight chelators, which can lead to the $H_2O_2$-dependent formation of hydroxyl radicals in the Fenton reaction:

$$O_2^- + Fe^{3+} (Cu^{2+}) \rightarrow Fe^{2+} (Cu^+) + O_2,$$

$$Fe^{2+} (Cu^+) + H_2O_2 \rightarrow Fe^{3+} (Cu^{2+}) + OH^- + {}^\cdot OH.$$
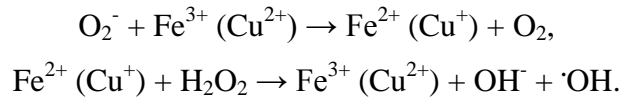
$O_2^-$ and $H_2O_2$ can react in the Haber-Weiss reaction to generate $^\cdot OH$ (*19*):

$$O_2^- + H_2O_2 \rightarrow {}^\cdot OH + OH^- + O_2.$$
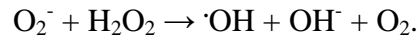
$^1O_2$ is an excited state of molecular oxygen that can be generated in a number of ways including the spontaneous dismutation of two $O_2^-$ radicals (*19*).

The oxidative burst reaction begins with the recognition of the elicitor molecule by a corresponding receptor molecule (*20*). Components of the signaling pathway downstream of the receptor may include heterotrimeric GTP-binding proteins (*4*). ROS generation appears to depend on increased intracellular $Ca^{2+}$ level. ROS signal transduction further activates $Ca^{2+}$ channels and induce cytosolic $Ca^{2+}$ increases in plant cells. Ion fluxes cause transient alkalinization of the extracellular matrix in the apoplast, leading to the activation of pH-dependent cell wall peroxidase, forming $H_2O_2$ (*20*). $NO^{3-}$ efflux seems to be essential to induce NADPH oxidase (*12*). Also protein phosphorylation may trigger the ROS signaling (*4*). Cyclic AMP-signaling system may also be an upstream event in the ROS signaling by leading to the activation of NADPH oxidase (*20*).

ROS induce SA, jasmonate, and various defense responses, including strengthening of plant cell walls by a peroxidase-catalyzed cross-linking of cell wall structural proteins and triggering the transcription of defense-related genes. (*4*). $O_2^-$ triggered defense gene activation and phytoalexin synthesis in parsley and during the barley-powdery mildew interaction ROS induced the hypersensitive reaction.

## 2.6 Nitric oxide in signal transduction

NO is a gaseous free radical that diffuses readily through biomembranes (*4*). It is involved both in the animal and the plant defense signaling. NO production was observed in tobacco cells within 5 min after treatment with an elicitor cryptogein and maximum increase was observed within 30 min (*21*).

A mammalian enzyme NO synthase (NOS) converts L-arginine into L-citrulline in a NADPH-dependent reaction, releasing NO (*22*). Similar NO synthesis by a NOS-type enzyme also occurs in plants. This pathogen-inducible enzyme activity has been identified as a variant of the P protein of glycine decarboxylase complex and named variant P (*4*). Despite the lack of sequence homology with the animal NOS, the variant P exhibits a high level of NOS-like activity and

displays biochemical features similar to those of its animal counterparts. Remarkably, the cryptogein-elicited burst of NO in tobacco cells was reduced by NOS inhibitors (*21*).

Plants also synthetize NO from nitrite, either enzymatically by nitrate reductase that catalyzes the NAD(P)H-dependent reduction of nitrite to NO, or in a nonenzymatic manner (*4*). Nitrite-dependent NO production has been observed in soybean and sunflower.

NO synthesis is tightly regulated by a signaling cascade involving $Ca^{2+}$ influx and phosphorylation events (*21*). NO acts through a cGMP-dependent pathway, where it posttranslationally activates guanylate cyclase, which leads to a transient increase in cGMP that activates ADP-ribosyl cyclase through a cGMP-dependent protein kinase (*23*). This results in elevated levels of cyclic ADP ribose (cAPDR), which was shown to activate expression of several defense genes. NO has been shown to convert the cytosolic aconitase into an mRNA-binding protein known as iron regulatory protein-1 (IRP-1) in mammals (*23*). IRP-1 regulates free iron concentrations and through this mechanism NO stimulates increased levels of intracellular free iron. In the presence of ROS, free iron promotes oxidative damage via the Fenton reaction and contributes to induction of the hypersensitive reaction in plants (*4*). NO increases SA levels in elicitor-treated cells. SA is critical for cADPR-mediated activation of *PR1* expression, but not for the cADPR-mediated activation of *PAL* expression (*23*). Thus, NO appears to regulate expression of various defense genes through either SA-dependent or -independent pathway. NO was shown to activate SIPK in tobacco most probably via a SA-dependent pathway (*4*). Remarkably, NO inhibited the $H_2O_2$-scavenging enzymes catalase and ascorbate peroxidase activities in tobacco, which suggests NO may participate in redox signaling and plays a role in regulating $H_2O_2$ levels. Last but not least, NO appears to be also involved in the pathway leading to the accumulation of transcripts encoding the ET-forming enzyme and cell death (*21*).

## 2.7    Salicylic acid-signaling system

SA is a signal molecule that acts both locally in intracellular and systemically in intercellular signal transduction (*24*). It accumulates in plants inoculated with pathogens (*4*). The increased levels of SA resulted in induction of various defense-related genes. The NPR1 (nonexpressor of *PR1*) protein is stimulated by SA to translocate to the nucleus where it interacts with TGA transcription factors, leading to the expression of various defense-related genes. SA was shown to regulate the expression of several *PR* genes encoding antimicrobial proteins. SA accumulation was suggested to be required for the hypersensitive reaction to occur and to contribute to disease

resistance (*25*). SA may play a key role in transferring intracellular signal transmitted by $Ca^{2+}$ (*4*).

Plants synthesize SA by the action of phenylalanine ammonia lyase (PAL) and the biosynthesis of SA is stimulated by high $H_2O_2$ levels and by phosphorylation modulating GTP-binding proteins (*4*). SA suppresses the $H_2O_2$-degrading activity of catalase and ascorbate peroxidase. SA has been shown to inhibit catalase by serving as a one-electron donating substrate (*26*). In this process, SA is converted into a free radical, which could then initiate lipid peroxidation. Lipid peroxides are potent signaling molecules and induce e.g. *PR1* genes (*4, 26*). Remarkably, two SA-binding proteins (SABPs) have been identified: a catalase, termed just SABP, and a lipase, termed SABP2 and generating a lipid-derived signal (*4*).

## 2.8    Jasmonate-signaling pathway

Jasmonates (JAs) are a major group of signaling compounds in inducing host defense (*27*). They are derived from peroxidized linolenic acid and are members of a large class of oxygenated lipids called oxylipins (*4*). JA induces a number of proteins, most of which are of unknown function, but some may have antimicrobial activity (*28*). The activated defense genes include e.g. genes encoding PAL, plant defensin, proteinase inhibitors, several secondary metabolites, basic chitinase and PR4 (*4*). JA and MeJA induce resistance against various pathogens. It was suggested that JA and MeJA may be involved in intercellular signaling. The components of JA-signaling pathway include phosphorylation and $Ca^{2+}$ influx.

## 2.9    Ethylene-dependent signaling pathway

The increased production of ET is one of the earliest events in pathogen-infected plants (*4*). The role of ET in plant-pathogen interaction is complex (*29*). Depending on the type of pathogen and plant species, ET may induce susceptibility or disease resistance. Through its signaling system, consisting of a histidine kinase and a response regulator protein, ET induces several *PR* and other defense-related genes (*4*).

## 2.10    Abscisic acid signaling

During fungal infection, ABA accumulates in the infected tissues (*4*). ABA may be a key factor in systemic induction of proteinase inhibitor genes. ABA functions as a negative regulator of

SA-dependent defense responses and confers susceptibility to diseases. Through the action of JIN1, a transcriptional activator and a positive regulator of ABA signaling in *Arabidopsis*, ABA also inhibited ET- and JA-signaling pathways (*30*).

## 2.11 Interplay of signaling pathways

Plant responses to different environmental stresses are achieved through integrating shared signaling networks and mediated by the synergistic or antagonistic interactions with the phytohormones SA, JA, ET, and ABA (*31*). Cross-communication between defense signaling pathways provides the plant with an elaborate regulatory potential that leads to the activation of the most suitable defense against the invader encountered (*32*). How particular stresses are decoded and translated to provide the output specificity remains largely unknown (*31*).

In *Arabidopsis*, responses to different pathogens have been shown to include a synergistic effect of JA and ET for induction of defense-related genes (*4*). ET-responsive factors play important roles in regulating JA-responsive gene expression, possibly via interaction with the GCC-box. ET and JA pathways may converge in the transcriptional activation of *ERF1*, which encodes a transcription factor regulating the expression of pathogen response genes that prevent disease progression. It has been shown that both ET and JA pathways are required simultaneously to activate *ERF1*. Probably, *ERF1* is a key element in the integration of ET and JA signals for the regulation of defense response genes.

Plant resistance to biotrophic pathogens is classically thought to be mediated through SA signaling (*31*). By contrast resistance to necrotrophic pathogens is controlled by JA and ET signaling pathways and genetically, SA and JA/ET defense pathways interact antagonistically. SA produced during pathogen infection plays an important role in the suppression of both JA biosysnthesis and JA-responsive gene expression (*32*). The SA-mediated inhibition of JA formation might be the result of a coordinated suppression of JA-responsive genes encoding enzymes of the octadecanoid pathway, including *LOX2*. NPR1 has been demonstrated to be an important transducer of the SA signal in the SA-mediated activation of *PR* gene expression and broad-spectrum resistance. NPR1 was found to interact with members of the TGA subclass of the bZIP transcription factor family. TGA factors specifically bind to TGACG motifs. Interestingly, all JA-responsive genes tested to day contain one or more TGACG motifs in their promoters. Therefore, it was hypothesized that NPR1-TGA interactions might play a role in the SA-mediated suppression of JA-responsive genes. According to the proposed model, NPR1 is translocated to the nucleus upon activation by SA, where it facilitates the activation of SA-

responsive *PR* genes, and in the cytosol, the remaining SA-activated NPR1 pool is involved in the suppression of JA-responsive gene expression, either by facilitating the delivery of negative regulators of JA-responsive genes to the nucleus or by inhibiting positive regulators of JA-responsive gene expression.

Interplay between ET and SA-dependent pathways has been reported in some instances (*4*). ET may potentiate SA-mediated *PR1* gene expression, which might be negatively regulated by EDR1 protein.

A complex interplay between ABA- and JA-dependent pathways has been reported (*4*). Exogenous ABA suppressed both basal and JA-activated transcription of defense genes. ABA may also suppress ET-signaling system in plants. It has been demonstrated that the ET-insensitive *Arabidopsis* mutants show increased sensitivity to ABA, suggesting that ET signaling antagonizes ABA-responsive gene expression. It also has been shown that ABA suppresses SA accumulation in plants during interactions with pathogens (*31*).

## 3.    <u>Inducible plant defense responses</u>

The plant defense responses induced after successful recognition of the invading pathogen can be assigned to three major categories, according to their distinct temporal and spatial expression patterns (*33*):

1. Immediate, early defense responses – initiated in the directly invaded plant cell and the neighboring cells, frequently leading to the hypersensitive response (HR).

2. Subsequent local activation of genes in vicinity of infection, including *de novo* synthesis of proteins involved in the formation of antimicrobial phytoalexins, structural proteins incorporated into the cell wall, and various protective proteins.

3. Delayed systemic activation of genes encoding PR proteins, which are directly or indirectly inhibitory toward pathogens, resulting in the establishment of immunity to secondary infections termed systemic acquired resistance (SAR).

### 3.1    The hypersensitive response

The term hypersensitive response was introduced by Stakman as early as 1915 to describe the rapid and localized cell death associated with cereal resistance to the rust fungus *Puccinia graminis* (*33*). Subsequently, the HR was recognized as a general defense reaction in numerous plant-pathogen interactions. It is associated with plant disease resistance and occurs nearly

ubiquitously in incompatible plant-pathogen interactions. HR is a kind of programmed cell death (PCD) and is associated with many morphological and biochemical changes, such as change in the appearance of the plant cell nucleus, the cessation of cytoplasmic streaming, the appearance of particles exhibiting Brownian motion within the vacuole, protoplast collapse, degradation of host DNA into oligonucleosomal fragments, terminal deoxynucleotidyltransferase-mediated UTP end labeling-positive cells, caspase-like activities, cytochrome *c* release or cleavage of poly (ADP-ribose) polymerase (*4, 33*). In general, plant cells dying during the HR show several but not all hallmarks characteristic of animal PCD (*33*). The possible pathway in induction of hypersensitive cell death is presented in Figure 3.
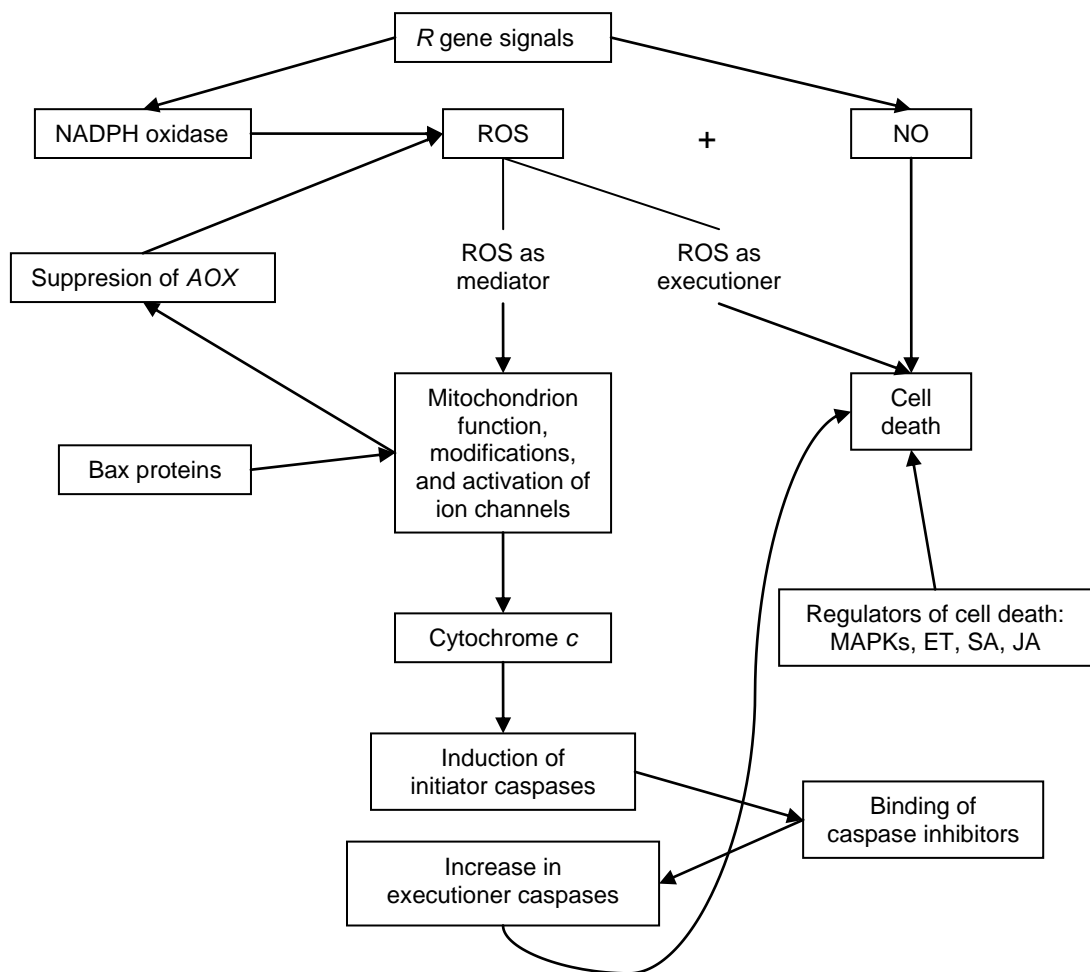


**Figure 3**: Suggested pathways in induction of hypersensitive cell death (*4*). ROS = reactive oxygen species, AOX = alternative oxidase, Bax = BCL2-associated X protein, ET = ethylene, SA = salicylate, JA = jasmonate.

HR may restrict invasion of biotrophic pathogen beyond the point where cell death occurs by depriving pathogens of water and nutrients (*34, 35*). Dying cells may release toxic compounds upon self-destruction and inhibit growth of pathogen (*36*). It appears that dying cells may be able to release signals to trigger local and systemic resistance (*4*). Diffusible signals eliciting *PR* gene

expression in cells neighboring HR cell death have been reported in many cases. The cell death is known to activate SA accumulation, which is involved in SAR development.

Cell death may also be induced in susceptible interactions (*4*). This cell death is called susceptibility-related cell death or normosensitive cell death and may be involved in conferring susceptibility to necrotrophic pathogens. Susceptibility-related cell death may provide nutrients for necrotrophic pathogens and shows characteristics of apoptosis, similar to that observed in resistance-related cell death.

## 3.2    Secondary metabolites in plant defense

Most of the plant secondary metabolites show antifungal action (*4*). There are two types of antifungal secondary metabolites: phytoalexins, that are inducible and synthesized *de novo* in response to infection, and phytoanticipins, that are constitutive and preformed infectional inhibitors. Both of them have been shown to be involved in disease resistance, although they have been detected in both resistant and susceptible interactions (*37*). Some compounds may be phytoalexins in one plant species and phytoanticipins in others.

Transcriptional activation of enzymes involved in biosynthesis of phytoalexins has been observed within a few minutes after the recognition of pathogen invasion (*4*). Induction of phytoalexin synthesis is delayed in susceptible interactions when compared with that in resistant interactions. The synthesized phytoalexins may be secreted from the cells (*38*). Phytoalexins have been reported to be highly fungitoxic, inhibitory to fungal spore germination and hyphal growth (*4*). They may also suppress toxin production by the pathogens.

Phytoalexins constitute a chemically heterogenous group of substances, such as phenylpropanoids, terpenoids, indole compounds, alkaloids, nitrogen-containing compounds, and fatty acid derivative compounds (*4*). Phytoanticipins are low-molecular weight and belong to several chemical classes including phenolic acids, di- and trihydroxy phenolics, flavanones, flavonoids, isoflavones, isoflavonoids, isoflavans, isoflavanones, glucosides of isoflavonoids, pterocarpans, furanocoumarins, anthocynidins, chromene, bibenzyl, xanthone, benzoxazinone, terpenoid saponins, steroid saponins, steroidal glycoalkaloid saponin, dienes, glucosinolates, and cyanogenic glucosides.

## 3.3 Pathogenesis-related proteins

Pathogenesis-related proteins (PRs) are defined as proteins encoded by a host plant's genome that are induced specifically in pathological situations (*4*). PRs are also induced upon environmental stresses, by chemical elicitors, and at different developmental stages of the plant (*39*). The proteins expressed constitutively in healthy plants and others expressed during specific developmental stages, such as flowering, have been referred to as PR-like proteins (*40*). Interestingly, some proteins induced by pathogens in one type of plant organ have been found to be constitutive components in other organs (*4*). Furthermore, some PRs induced in some varieties occur constitutively in other varieties. Even in the same plant, PRs appearing in lower old leaves without any stress were detected only after pathogen induction in young leaves near the top of the tobacco plant.

Some PRs have been shown to have antifungal activity and may be involved in reinforcement of host plat cell wall and induction of disease resistance (*4*). Many transgenic plants overexpressing PRs showed enhanced disease resistance. However, there are also reports that some of these transgenic plants overexpressing PRs did not show any enhanced disease resistance. Some of the PRs accumulate more in susceptible interactions and several PRs do not have any toxic action against pathogens. These observations suggest that not all, but some specific PRs may be involved in conferring disease resistance.

The accumulation of PRs after pathogen invasion occurs both locally and systemically and in both susceptible and resistant interactions (*41*). SA, JA, and ET may activate transcription of different sets of PRs and it is well established that different signal transduction systems are involved in induction of PRs (*4*). In tobacco plants, SA induces the expression of at least nine different *PR* genes and interestingly, all of them were also induced by tobacco mosaic virus (*42*). With mutants with impaired ET or JA pathways enhancement of resistance was observed (*39*). Apart from the effects of the signal molecules acting individually, there exists the possibility of synergism or antagonism among signal molecules on expression of PRs. For example, accumulation of PR-5 mRNA was dramatically higher in tobacco leaf tissues when ET and SA were applied in combination compared to plants with either one alone. Exogenous application of various chemicals could also induce the accumulation of PRs.

Structure of the PRs varies widely (*4*). PRs have been classified into 17 groups based on their structure and not based on their functions. The classification of PRs is summarized in the following table.

**Table I**: Classification of PR proteins (*4, 39*).

| Family | Biochemical properties / function | MW range [kDa] |
|---|---|---|
| PR-1 | Plant cell wall thickening | 15-17 |
| PR-2 | β-1,3-glucanase | 30-41 |
| PR-3 | Chitinase | 35-46 |
| PR-4 | Chitinase | 13-14 |
| PR-5 | Alteration of fungal membrane permeability | 16-26 |
| PR-6 | Proteinase inhibitor | 8-22 |
| PR-7 | Endoproteinase | 69 |
| PR-8 | Chitinase | 30-35 |
| PR-9 | Peroxidase | 50-70 |
| PR-10 | Ribonuclease | 18-19 |
| PR-11 | Chitinase | 40 |
| PR-12 | Alteration of ion transport in fungal membrane (defensins) | 5 |
| PR-13 | Thionin | 5-7 |
| PR-14 | Lipid transfer proteins | 9 |
| PR-15 | Germin-like oxalate oxidase | 22-25 |
| PR-16 | Germin-like proteins without oxalate oxidase activity | 100 (hexamer) |
| PR-17 | Peptidase | 27 |

Many of the PRs have signal peptide sequences at their N-termini, suggesting that these proteins are made on ribosomes attached to the endoplasmic reticulum, and it is very likely that the PRs are deposited in the lumen of the endoplasmic reticulum, where they are then transported to other locations, including secretory vesicles (*39*). Acidic PRs have been identified in the apoplastic fluid of plant cells, whereas basic PRs are rather found to accumulate in the vacuoles. Sequence analyses of cDNA clones of the encoded basic PRs have indicated the presence of additional sequences at the C-termini, which have been shown necessary and sufficient for targeting to the vacuoles. In some cases, the vacuolar targeting signal may be found at the mature N-terminus (*43*). Interestingly, many basic (intracellular) forms of PRs have been shown to have strong antifungal activity *in vitro*, in contrast to their acidic (extracellular) forms (*39*). Remarkably, the fungal pathogens initially develop in the intercellular space and subsequently grow extracellulary in the necrotrophic phase. Thus, basic (intracellular) forms of PRs practically have little effect on the fungal hyphae, despite having strong antifungal activity *in vitro*.

The defensive role of β-1,3-glucanases (PR-2 family) and chitinases (PR-3, -4, -8, -11 families) against fungal pathogens consists in either direct degradation of pathogen cell walls or in promotion of the release of cell wall-degradation products, which can further elicit a wide range of defense reactions. Proteinase inhibitors (PR-6 family) inactivate some pathogen proteinases and thus may reduce the ability of the pathogen to digest host proteins (*39*). Some thaumatin-like proteins (TLPs, PR-5 family) also have β-1,3-glucanase activity (*44*), while other TLPs work via

a mechanism involving mitogen-activated protein kinases, leading to changes in the fungal cell wall (*45*). Peroxidases (PR-9 family) are key enzymes in the cell wall building process, and it has been suggested that extracellular or wall-bound peroxidases could enhance plant resistance (*46*). Even though many peroxidases are expressed constitutively in plants, some isozymes appear to be inducible upon pathogen infection. Germin-like proteins (PR-15 and -16 families) may generate hydrogen peroxide, which is involved in cell wall cross-linking (*47, 48*). A role for NtPRp27 (PR-17 family) in plant defense has been proposed in previous studies, because the finding that the level of *NtPRp27* transcripts increased on tobacco mosaic virus infection and mechanical wounding, as well as after drought and ABA treatments, provided a profile that satisfies the definition of a PR protein (*49*). Cyclophilins catalyze *cis-trans* isomerization of imide bonds in peptides and proteins and may be implicated in protein folding and in long-range interaction between cells (*50*). Cyclophilin-like antifungal proteins have been isolated from black-eyed pea (*51*), mungbean (*52*), and chickpea (*53*).

## 4.      **Cryptogein**

Cryptogein is a very efficient elicitin from *Phytophthora cryptogea* (*8*). It is synthesized as a pre-protein with a signal peptide removed co-translationally before the secretion, accumulating in its mature form in the mycelium (*4*).

The three-dimensional structure of cryptogein was determined by crystallography and NMR (*54, 55*). It is composed of five α-helices and one β-sheet arranged in a unique protein fold. A hydrophobic cavity is located in the protein core and connected with the protein surface by a tunnel.

Cryptogein and elicitins generally are structurally similar to lipid-transfer proteins of plant cells (*56*). They behave like sterol carrier proteins (*57*) and are able to pick up sterols from plasma membranes (*58*). The original proposal that elicitins may facilitate transfer of sterols was corroborated by the crystal structures of cryptogein in complex with dehydroergosterol (DHE) and cholesterol (*7*). The biological role of elicitins has been suggested to be the storage and transport of sterols used by *Phytophthora* spp. (*8*).

Specific binding of cryptogein to a high-affinity binding site on the tobacco plasma membrane, a putative cryptogein receptor composed of a calcium channel and a glycoprotein, has been reported (*59*). This plasma membrane component is a heterodimeric *N*-glycoprotein with subunits of 162 and 50 kDa.

Application of cryptogein to tobacco cells triggered depolarization of the plasma membrane, protein phosphorylation, cytosol acidification and alkalinization of the extracellular medium, concomitant potassium and chloride efflux, fast and large influx of calcium, transient production of ROS as a consequence of plasma membrane NADPH oxidase activity induction, cell wall modifications, pentose phosphate pathway, MAPK activation, disruption of the microtubular cytoskeleton, NO production, production of ethylene, and induction of defense-related genes (*4, 7, 8*). These early events could be prevented by the treatment of cells with calcium channel inhibitors, phospholipase C inhibitors or by the inhibition of protein kinases by staurosporin, indicating that phosphorylation reactions occurred upstream from these effects (*60*). On the basis of studies using the inhibitors, it was suggested that cryptogein-induced signal pathway leading to the oxidative burst and ΔpH changes includes phospholipase C together with protein kinase C (*61*). The late events include synthesis of phytoalexins such as capsidiol together with expression of defense related genes covering PR proteins. As well, the cell necroses could be observed as a consequence of hypersensitive response (*62*).
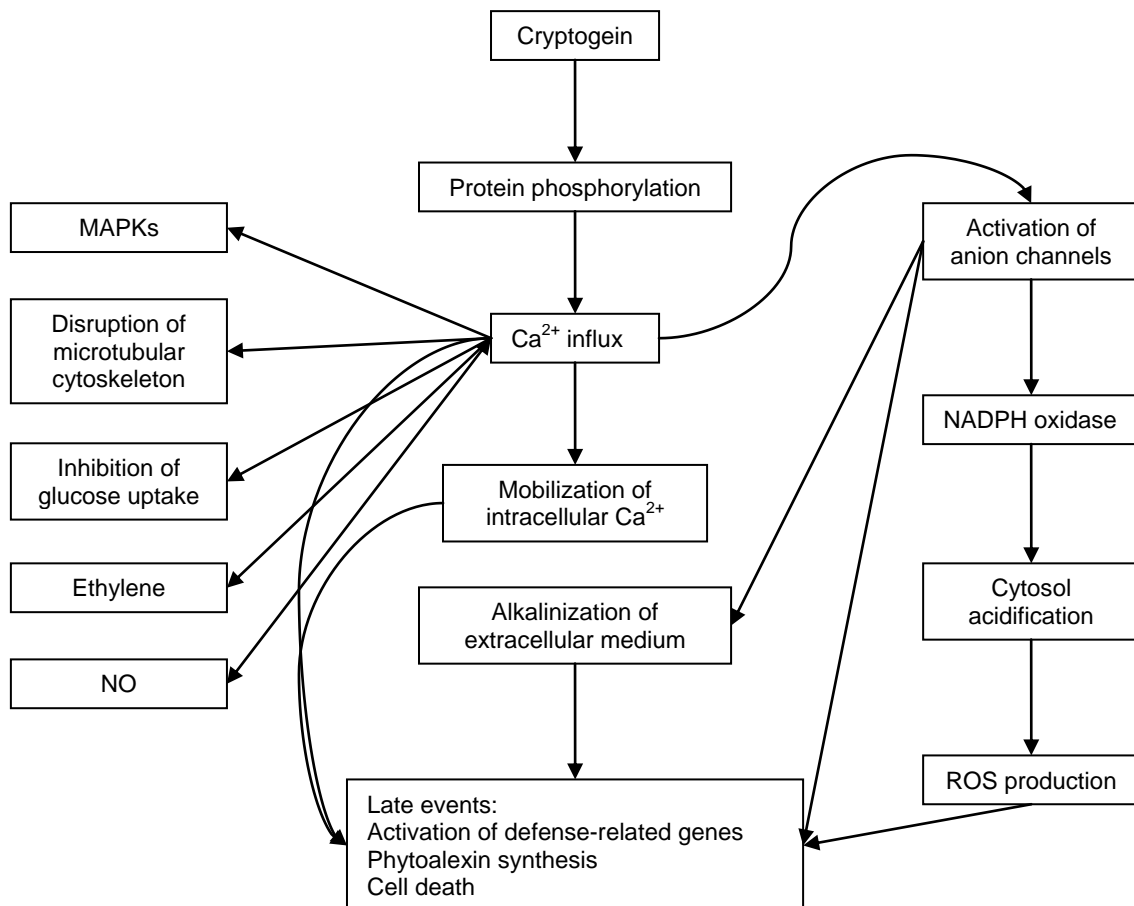


**Figure 4**: Cryptogein in induction of various signal transduction systems in tobacco (*4*).

The expression of PR proteins and the induction of local acquired resistance were observed after the treatment of leaves with cryptogein (*8*). Distribution on the stem of decapitated plants is followed by rapid translocation of cryptogein and the plant becomes resistant to further inoculation by pathogens. Other cultivated *Solanaceous* genera (petunia, pepper, and tomato) did not develop any leaf necrosis and protection in response to cryptogein.

The link between elicitor and sterol-loading properties is still not clear, but there are several works trying to explain it using site-directed mutagenesis. The cryptogein residues Tyr47 and Tyr87 were suggested to be involved in sterol binding (*63*). With the use of site-directed mutagenesis of these residues, the mutated cryptogeins were strongly altered in their sterol-binding efficiency, specific binding to high-affinity sites, and activities on tobacco cells. The formation of a sterol-elicitin complex is probably a prerequisite step before elicitins fasten to specific binding sites.

Another work deals with multiple mutations of the residues L15, L19, M35, L36, M59, and I63 directed mainly into the hydrophobic cavity (*8*). The far-UV-CD spectra of all mutants were similar to the spectrum of the wild type so that the mutations did not perturb markedly their structure. In that study, all recombinant cryptogeins were tested for their ability to bind DHE and *cis*-parinaric acid. Both lipids only slightly fluoresce in water due to self-quenching of the fluorescent molecules in lipid micelles. After the lipids bind into the elicitin's central cavity, their fluorescence markedly increases (*64*). Also the effects of site-directed mutagenesis on the synthesis of ROS and changes of extracellular pH in suspension tobacco cells induced by cryptogeins were measured in this work (*8*).

The results that are summarized in Table II showed that the ability to induce the synthesis of ROS and pH changes is linked to the ability to bind sterols and not fatty acids (*8*). The computer modeling showed that DHE binding initiates conformation changes of the ω loop and consequently overall protein structures. Fatty acids did not stimulate such changes. They could accommodate the shape of the cavity because of their flexibility (*7*). The ω loop is very flexible and highly conserved. Its conservative structure suggests an important function (*8*). Proteins L15W/L36F and M35W/M59W did not bind sterols, but remained efficient to induce the early events. Both proteins contain bulky residues in the ω loop (W35, F36). Such a big residue directed inside the structure must be compensated by conformation changes in the ω loop that are very similar to those induced by the binding of sterols. The results suggest that the conformation of the ω loop induced either by sterol binding or by the presence of bulky residues could be necessary for the ability to trigger the early events caused by cryptogeins.
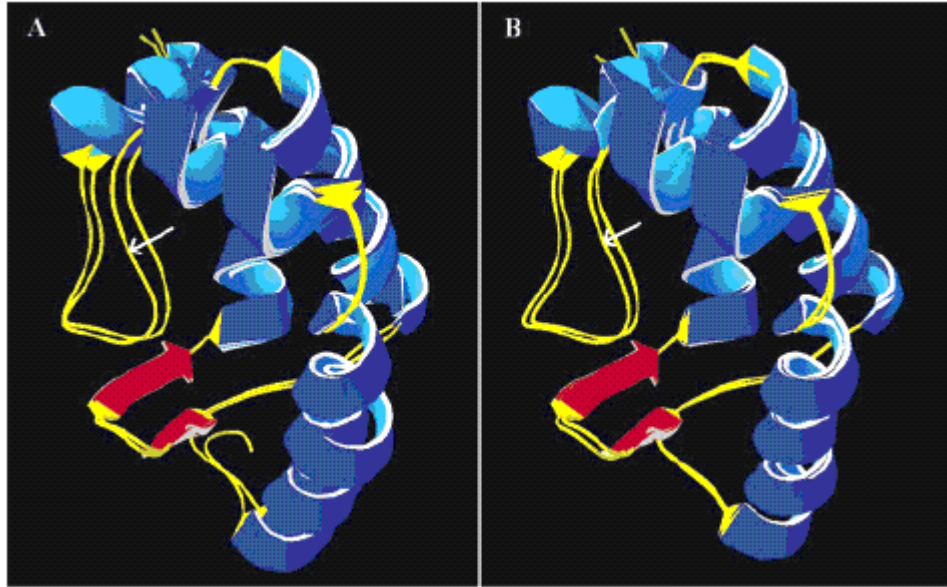
**Figure 5**: Superposition of the free wild type, dehydroergosterol-bound wild type, and mutant structures of cryptogein. (A) Binding of dehydroergosterol to the cavity of cryptogein wild type induces a conformational change in the ω loop (arrow). (B) Superposition of the structures of wild type and the M35W/M59W mutant (arrow) of cryptogein. Changes induced by the mutation are similar to those induced by sterol binding. Proteins are represented as ribbons; α-helices in blue, β-strands in red, and loops in yellow (*8*).

All the mentioned mutated cryptogeins were able to stimulate necroses of suspension tobacco cells and to express the defense proteins, independently on their abilities to bind sterols or to stimulate the synthesis of ROS and pH changes (*8*). The ability to express PR proteins and to induce cell necroses depends probably rather on overall structure of the elicitins and charge distribution. These results further suggest that elicitins could activate two signal pathways that may not be necessarily connected.

**Table II**: Dissociation constants of complexes of dehydroergosterol (DHE) and *cis*-parinaric acid (CPA) with mutated cryptogeins and biological effects of mutants (*8*).

| mutation | $K_d$ (µM) | | ROS synthesis | pH change |
|---|---|---|---|---|
| | **DHE** | **CPA** | | |
| wild type | $0.50 \pm 0.02$ | $0.19 \pm 0.01$ | +++ | +++ |
| M35F/M59W | $0.21 \pm 0.01$ | $0.132 \pm 0.007$ | ++ | +++ |
| M35F/M59W/I63F | $0.68 \pm 0.05$ | $0.09 \pm 0.01$ | +++ | +++ |
| M35W/M59W | no binding | $0.08 \pm 0.01$ | + | ++ |
| L19R | no binding | $0.12 \pm 0.02$ | no effect | no effect |
| L15W/L36F | no binding | no binding | + | ++ |

Elicitins are also known to bind fatty acids to the internal cavity, making them functionally similar to the family of plant lipid transfer proteins, although this affinity is significantly lower (*58, 63*). Interestingly, plant lipid transfer proteins can associate with the same receptor in

tobacco as elicitins and they can bind fatty acids and phospholipids but not sterols (*56*). Fatty acids bound to the cavity interact mainly with the residues making up the groove: Y33, P42, Y47, L41, V75, L80, L82, and Y87 (*7*). Unlike sterols, free fatty acids are not present in noticeable amounts in membranes, but can be liberated by the action of phospholipase A1 and A2. The relationship between the complexation of elicitin with sterol and fatty acid is currently unknown and the design of protein mutants selectively binding either molecule can stimulate future research.

Geranylgeranyol and farnesol are widespread in plant and animal cells in a form of prenylated proteins (*7*). These covalently attached lipids are recognized as being critically important for cellular signaling processes. It was shown that geranylgeranyol and farnesol bind to the elicitins as efficiently as the most strongly binding fatty acids. The importance of these interactions with elicitins or plant lipid transfer proteins for the cell signaling should be tested.

Substitution of the residues M59, I63, or V84 by a large hydrophobic amino acid, e.g. phenylalanine or tryptophan, should reduce binding of sterol to the cavity of cryptogein (*7*). These mutations should not have an effect on the binding of fatty acids, farnesol and geranylgeranyol, filling a free space next to the molecules bound in the groove. Substitution in the position I63 is the most suited for this purpose, because it is located right to the groove of protein. The I63 residue is absolutely conserved among all currently known elicitins (*8*). Substitution of the amino acid residues L41 and L80 for larger hydrophobic amino acids should distinctively decrease binding of fatty acids, farnesol, and geranylgeranyol in the groove of the cavity, while preserving the binding of sterol (*7*).

## 5. *In vitro* site directed mutagenesis

*In vitro* site directed mutagenesis is an invaluable technique for characterizing complex relationships between protein structure and function and for carrying out vector modification (*65*). The basic procedure utilizes a DNA vector with an insert of interest and two synthetic oligonucleotide primers, both containing desired mutation. The oligonucleotide primers, each complementary to opposite strands of the vector, are extended during temperature cycling by a special DNA polymerase, without primer displacement. Extension of the oligonucleotide primers generates a mutated plasmid containing staggered nicks. Following temperature cycling, the product is treated with *Dpn*I endonuclease, which digests methylated and hemimethylated DNA corresponding to parental DNA template.

## 6.    Heterologous protein expression in *Pichia pastoris*

Yeasts were the first eukaryotic cells engineered to express heterologous proteins because they share with *E. coli* many of the characteristics that make the latter such a useful host for recombinant DNA technology (*66*). They grow rapidly, can be transformed as intact cells, and form discrete colonies. In addition, they can carry out post-translational modifications of expressed proteins that *E. coli* is unable to provide. Furthermore, they secrete a small number of proteins into the growth medium, which can be exploited to simplify the purification of heterologous proteins. Finally, unlike *E. coli*, yeasts do not produce pyrogens or endotoxins.

*Pichia pastoris* is a methylotrophic yeast, disposing of a specific biochemical pathway that allows it to utilize methanol as a sole carbon source (*66*). The promoters of the genes that encode the enzymes for this pathway are extremely strong and exquisitely sensitive to the presence or absence of methanol, making them ideal for the regulation of heterologous gene expression. *Pichia pastoris* have a number of advantages over ethanol-producing yeasts. It grows to much higher densities in fermenters due to the absence of toxic levels of ethanol, uses integrative vectors, which removes the need for selective media, offers greater mitotic stability of recombinant strains, and has a more authentic type of glycosylation pattern for heterologous products. Selection of transformants for heterologous gene expression commonly relies on complementation of an auxotrophic *his4* marker in the host cells. The gene of interest is spliced between the promoter and terminator sequences of the *AOX1* gene in *E. coli* vector, which also carries the *His4*$^+$ and further downstream of this the 3´ end of the *AOX1* gene. A linear fragment bounded by AOX1 sequences is then transformed into a *His4*$^-$ host. This DNA construct can then undergo homologous recombination targeting the gene of interest into the chromosomal locus of the *AOX1* gene. Another possibility to select positive transformants can be based on zeocin resistance or *ade2* auxotrophic marker. The cells can grow either on methanol, in which case the heterologous protein is continuously expressed, or on glucose, in which case the heterologous gene is repressed until induced by methanol. The *Saccharomyces cerevisiae* α-factor prepro sequence is the most widely used secretion signal sequence. It is usually genetically egineered onto the DNA sequence for the heterologous protein of choice, thereby ensuring that it is targeted for export into the culture medium after being synthesized.

## 7. <u>Two-dimensional electrophoresis</u>

Two-dimensional (2-D) electrophoresis is a powerful and widely used method for the analysis of complex protein mixtures extracted from biological samples (*67*). This technique sorts proteins according to two independent properties in two discrete steps: the first-dimension step, isoelectric focusing (IEF), and the second-dimension step, SDS-polyacrylamide gel electrophoresis (SDS-PAGE).

### 7.1    First dimension separation: IEF

Proteins are first separated on the basis of their pI, the pH at which a protein carries no net charge and will not migrate in an electrical field and is determined by the number and types of charged groups in a protein (*68*). The technique is called isoelectric focusing (IEF). For 2-D electrophoresis, IEF is best performed in an immobilized pH gradient (IPG).

When a protein is placed in a medium with a pH gradient and subjected to an electric field, it will initially move toward the electrode with the opposite charge (*68*). During migration through the pH gradient, the protein will either pick up or lose protons. As it migrates, its net charge and mobility will decrease and the protein will slow down. Eventually, the protein will arrive at the point in the pH gradient equal to its pI. There, being uncharged, it will stop migrating. If this protein should happen to diffuse to a region of lower pH, it will become protonated and be forced back toward the cathode by the electric field. On the other hand, if it diffuses into a region of pH greater than its pI, the protein will become negatively charged and will be driven toward the anode. In this way, proteins condense, or are focused, into sharp bands in the pH gradient at their individual characteristic pI values. pH gradients for IPG strips are created with sets of acrylamido buffers, which are derivatives of acrylamide containing both reactive double bonds and buffering groups. The general structure is $CH_2=CH–CO–NH–R$, where R contains either a carboxyl [–COOH] or a tertiary amino group (e.g. $–N(CH_3)_2$). These acrylamide derivatives are covalently incorporated into polyacrylamide gels at the time of casting and can form almost any conceivable pH gradient.

Commercial IPG strips are dehydrated and must be rehydrated to their original gel thickness (0.5 mm) before use (*68*). As the strips hydrate, proteins in the sample are absorbed and distributed over the entire length of the strip. After the strips rehydrated, they are moved to the IEF focusing tray. A wet wick is placed on each electrode to collect salts and other contaminants

in the sample. The strips are covered with mineral oil before starting the focusing run to prevent evaporation and carbon dioxide absorption during focusing.

## 7.2    Second dimension separation: SDS-PAGE

Second-dimension separation is by protein mass, or MW, using SDS-PAGE (*68*). The pores of the second-dimension gel sieve proteins according to size because dodecyl sulfate coats all proteins essentially in proportion to their mass. The net effect is that proteins migrate as ellipsoids with a uniform negative charge-to-mass ratio, with mobility related logarithmically to mass.

To solubilize focused proteins and to allow SDS binding in preparation for the second dimension, it is necessary to equilibrate focused IPG strips in SDS-containing buffers (*68*). After equilibration strips are embeded onto the SDS-PAGE second-dimension gel and overlayed with warm molten agarose prepared in SDS-PAGE running buffer, with a small amount of bromophenol blue in order to track the ion front during the run.

## 7.3    Proteins detection, image acquisition and analysis, and proteins identification

It is most common to make proteins in gels visible by staining them with dyes or metals (*68*). Each type of protein stain has its own characteristics and limitations with regard to the sensitivity of detection and the types of proteins that stain best. Before 2-D gels can by analyzed with an image evaluation software system, they must be digitized. The most commonly used devices are camera systems, densitometers, phosphor imagers, and fluorescence scanners. After image analysis, most current protein identification depends on mass spectrometry of proteins excised from gels.

## *Goal of the thesis*

The thesis should broaden the current knowledge in the field of plant-pathogen interaction. Cryptogein, an elicitin from an oomycete *Phytophthora cryptogea*, and a plant *Nicotiana tabacum* will be used as a model. I will focus particularly on the relationship between elicitin-lipid interaction and plant defense reaction course.

With the use of *in vitro* site directed mutagenesis, cryptogein mutants with an altered ability to bind sterols and/or fatty acids will be prepared. Mutations types will be chosen according to conclusions of a study of Dobeš *et al.* (2004) (*7*). For recombinant proteins production, an expression system of a yeast *Pichia pastoris* will be used. Subsequently, tobacco leaves will be treated with cryptogein mutants and the differences in plant defense reaction course will be observed mostly from a proteomic approach. After apoplastic fluid isolation, where the majority of defense-related proteins are expected, 2-D electrophoresis of tobacco apoplastic proteins with subsequent MS identification of spots selected on the basis of PDQuest (Bio-Rad) analysis will be performed. Supplementary experiments, such as observing HR extent, tobacco secondary compounds analyses, analysis of defense genes transcription level, and fluorescence measurements of interaction between cryptogein mutants and lipids will also be realized.

The obtained results could mean important facts for both basic and applied research, for example in searching for alternative crop plants protection against phytopatogenic fungi and oomycetes.

## *Materials and methods*

### 1.  <u>Materials</u>

pPIC-X24 plasmid, which is pPIC9 (Invitrogen) into which X24 gene that encodes cryptogein was cloned, was available from previous studies (*63*). Wild type cryptogein was prepared in our laboratory previously (*8*). Cryptogein mutants L41F, V84F, and L41F/V84F were prepared as described below.



Comments for pPIC9:
8023 nucleotides

5′ *AOX1* promoter fragment: bases 1-948
5′ *AOX1* primer site: bases 855-875
α-Factor secretion signal(s): bases 949-1215
α-Factor primer site: bases 1152-1172
Multiple Cloning Site: bases 1192-1241
3′ *AOX1* primer site: bases 1327-1347
3′ *AOX1* transcription
       termination (TT): bases 1253-1586
*HIS4* ORF: bases 4514-1980
3′ *AOX1* fragment: bases 4870-5626
pBR322 origin: bases 6708-6034
Ampicillin resistance gene: bases 7713-6853

**Figure 6**: pPIC9 vector map (*65*).

Tobacco seeds (*Nicotiana tabacum* L. cv. *Xanthi*) were sown into peat soil and plants were grown in controlled conditions (22 °C, 16 h light, 6.000 lux, 80% hygrometry). The experiments were done with 8 weeks old plants.

Sterols and phospholipids, except nitrobenzoxadiazole-labelled phosphatidylcholine (NBD-PC) were purchased from Sigma and were dissolved in ethanol and chloroform, respectively. NBD-PC was purchased from Invitrogen and was dissolved in chloroform. Proteins were dissolved in water and stored at -20 °C.

## 2.   <u>**Site-directed mutagenesis**</u>

Specific mutagenesis of *PIC-X24* gene encoding cryptogein was performed with the use of the PCR-derived technique developed with the QuikChange II XL site-directed mutagenesis kit (Stratagene). Oligonucleotides designed to introduce the chosen mutations into the target codon are stated in Table III.

**Table III:** Sequences of the oligonucleotides used for mutagenesis of cryptogein.

| Mutation | Primers (5´ → 3´) |
|----------|-------------------|
| L41F | F*: ACG GCC AAG GCC TTC CCC ACC ACG GCG |
|      | R*: CGC CGT GGT GGG GAA GGC CTT GGC CGT |
| V84F | F*: CGG CCT GGT ACT CAA CTT CTA CTC GTA CGC GAA CG |
|      | R*: CGT TCG CGT ACG AGT AGA AGT TGA GTA CCA GGC CG |

* F is the forward primer and R is the reverse primer, respectively.

PCR amplifications were carried out with 10 ng of PIC-X24 plasmid vector, 125 ng of each forward and reverse primer, 100 μM deoxyribonucleotide triphosphate mixture, and 2.5 U of *Pfu* DNA polymerase in a final volume of 50 μl. The cycling parameters are outlined in Table IV.

**Table IV:** Cycling parameters for the QuikChange II XL method.

| Segment | Cycles | Temperature | Time |
|---------|--------|-------------|------|
| 1 | 1 | 95 °C | 1 min |
| 2 | 18 | 95 °C | 50 s |
|   |    | 60 °C | 50 s |
|   |    | 68 °C | 8 min |
| 3 | 1 | 68 °C | 7 min |

The amplification mixture was subjected to *Dpn*I digestion (10 U, 37 °C, 1 h), where methylated and hemimethylated DNA corresponding to parental DNA template were digested. Subsequent molecules resistant to *Dpn*I digestion, corresponding to efficiently mutated DNA, were further cloned in *Escherichia coli* XL 10-Gold ultracompetent cells (Stratagene) by a heat shock method according to the manufacturer's recommendations. 100 μl of each transformation reaction was plated on LB-ampicilin agar plates and incubated at 37 °C for more than 16 h. Transformants were selected for their ability to grow in the presence of ampicillin (100 mg.l$^{-1}$), inoculated in 50 ml of LB liquid medium containing ampicillin (100 mg.l$^{-1}$), and incubated at 37 °C overnight. The culture was then centrifuged (6.000 x *g*, 15 min) and from the bacterial pellet plasmid DNA was isolated using the Plasmid Midi Kit (Qiagen), which is based on a modified alkaline lysis procedure, followed by binding of plasmid DNA to anion-exchange resin under appropriate low-

salt and pH conditions. RNA, proteins, dyes, and low-molecular weight impurities are removed by a medium-salt wash. Plasmid DNA is eluted in a high-salt buffer and then concentrated and desalted by isopropanol precipitation.

Correct orientation of the sequence was evaluated by DNA sequencing with primers FPIC9 and RPIC9 (for sequences see Table V) using BigDye Terminator v3.1 Cycle Sequencing Kit (Applied Biosystems), on 3100 Genetic Analyzer (Applied Biosystems). Positive clones were used to transform *Pichia pastoris* cells.

**Table V:** FPIC9 and RPIC9 primers sequences.

| Primer | Sequence (5′ → 3′) |
|--------|--------------------|
| FPIC9 | TAC TAT TGC CAG CAT TGC TGC |
| RPIC9 | GCA AAT GGC ATT CTG ACA TCC |

## 3. Transformation of *Pichia pastoris* and expression screen

The yeast *P. pastoris* strain GS115 was obtained from Invitrogen. Its propagation, as well as competent cell preparation and selection procedures, was according to the manufacturer's recommendations. pPIC-X24 and its mutants isolated as described above were linearized at the unique *Sac*I site in the vector and cloned into competent GS115 cells by a heat shock method according to the manufacturer's manual. Transformants were selected for their ability to grow on histidine-deficient MD agar plates. Eight selected transformants were inoculated in 5 ml of YPD liquid medium and incubated at 30 °C overnight. The culture was then plated on YPD agar plates and incubated at 30 °C for 2 days. Thereafter the culture was resuspended in 1 ml of expression medium (for composition see Table VI) and inoculated in 100 ml of expression medium into which 500 µl of biotin-methanol solution (1 mg of biotin in 1 ml of methanol) was added, and incubated at 30 °C for 4 days with the daily addition of 500 µl of methanol.

The efficiency of protein expression was then analyzed by SDS-PAGE and subsequent silver staining. The highest expressers were used for a large scale recombinant proteins production in a fermentor (for details see Master Thesis of Bc. Michal Obořil, FSc, MU).

**Table VI:** Expression medium final composition.

| component | content* | component | content* |
|---|---|---|---|
| Phosphate buffer, pH 6 | 0.2 M | Biotin | $1 \times 10^{-4}$ % (w/v) |
| $(NH_4)_2SO_4$ | 1 % (w/v) | Riboflavin | $5 \times 10^{-5}$ % (w/v) |
| $KH_2PO_4$ | 0.2 % (w/v) | Boric acid | $2 \times 10^{-6}$ % (w/v) |
| $MgSO_4.7H_2O$ | 0.205 % (w/v) | $CuSO_4.5H_2O$ | $2 \times 10^{-7}$ % (w/v) |
| NaCl | 0.02 % (w/v) | KI | $1 \times 10^{-5}$ % (w/v) |
| Calcium pantothenate | $1 \times 10^{-4}$ % (w/v) | $MnSO_4.H_2O$ | $3 \times 10^{-7}$ % (w/v) |
| Folic acid | $1 \times 10^{-6}$ % (w/v) | $Na_2MoO_4.2\ H_2O$ | $2 \times 10^{-5}$ % (w/v) |
| Inositol | $5 \times 10^{-4}$ % (w/v) | $ZnSO_4.7H_2O$ | $2 \times 10^{-6}$ % (w/v) |
| Nicotinic acid | $1 \times 10^{-4}$ % (w/v) | $CoCl_2.6\ H_2O$ | $1 \times 10^{-4}$ % (w/v) |
| p-aminobenzoic acid | $5 \times 10^{-5}$ % (w/v) | $CaCl_2.2H_2O$ | 0.026 % (w/v) |
| Pyridoxine HCl | $1 \times 10^{-4}$ % (w/v) | $FeSO_4.7H_2O$ | 0.06 % (w/v) |
| Thiamine HCl | $1 \times 10^{-4}$ % (w/v) | | |

* All components were dissolved in Milli-Q water. Biotin and riboflavin were pre-solubilized in 0.1 M NaOH.

## 4. Purification of recombinant proteins

The culture medium was centrifuged at 10.000 x *g* for 10 min at 4 °C. The supernatant was concentrated using Ultrafiltration Cell Model 202 (Amicon) and regenerated cellulose ultrafiltration membranes with cut-off 3000 Da (Millipore) to the volume of approximately 15 ml. The concentrate was extensively dialyzed against $H_2O$ (Milli-Q) for 48 h at 4 °C, adjusted to 5 mM sodium acetate buffer, pH 5.0. For protein separation, ÄKTA FPLC system (Amersham Pharmacia Biotech) was used. The sample was loaded onto a Tricorn 5/5 column (GE Healthcare) containing Source 15S ion exchange media (GE Healthcare) and equilibrated with 5 mM sodium acetate buffer, pH 5.0. The proteins were eluted with linear gradient of 5 mM sodium acetate buffer, pH 5.0, containing 1 M NaCl. The identity of expressed proteins was verified by MALDI-MS (Department of Functional Genomics and Proteomics, FSc, MU).

## 5. Tobacco apoplastic fluid isolation

Upper, middle, and lower leaves, each from a different tobacco plant (totally from 5 plants), were cut off and immerse in to the 250 nM cryptogeins solution. After 48 h the leaves were rinsed in water to remove any debris from the surfaces or cytoplasmic contaminants from the cut edges and vacuum infiltrated for 5 min at room temperature with an isolation buffer containing 25 mM Tris.Cl pH 7.8, 10 mM $CaCl_2$, 5 mM 2-mercaptoethanol, and 1 mM PMSF. The plant material was then blotted and rolled into the barrel of a 20 ml plastic syringe, which was

subsequently placed, hub down, in a 50 ml centrifuge tube and centrifuged at 800 x *g* for 10 min at 4 °C. The tobacco apoplastic fluid isolates collected at the bottom of the tubes were stored at -20 °C.

## 6.   Proteomic analysis

The tobacco apoplastic fluid isolates were concentrated using ultrafiltration devices (Vivaspin 6 Concentrator, GE Healthcare) with a 3 kDa cut-off by centrifugation at 8.000 x *g* at 4 °C, then rediluted in a sample buffer containing 8 M urea, 2% (w/v) CHAPS, 65 mM DTT, and 2% (v/v) IPG buffer (carrier ampholyte mixture, Bio-Rad) and reconcentrated using the same procedure. Finally the samples were diluted 10-fold with the sample buffer. The total protein concentration was determined with an *RC DC* Protein Assay Kit (Bio-Rad) using a calibration curve for BSA. For isoelectric focusing, Immobiline DryStrip pH 3-11 NL, 7 cm (GE Healthcare) IPG strips were used. Passive sample application during rehydration was performed. In each case, 80 μg of total protein in the sample buffer was loaded in triplicate. The rehydration time was 18 h. The IEF was performed using a PROTEAN IEF Cell (Bio-Rad). Focusing conditions are shown in Table VII. Before the SDS-PAGE procedure, the focused IPG strips were equilibrated, first in a DTT equilibration buffer [2% (w/v) DTT, 6 M urea, 2% (w/v) SDS, 0.05 M Tris.Cl pH 8.8, 20% (w/v) glycerol] for 15 min, then in an iodoacetamide equilibration buffer [2.5% (w/v) iodoacetamide, 6 M urea, 2% (w/v) SDS, 0.05 M Tris.Cl pH 8.8, 20% (w/v) glycerol] for 15 min. After equilibration, the IPG strips were embedded onto 12% acrylamide 1 mm SDS-PAGE second-dimension gels. SDS-PAGE was performed using a Mini-PROTEAN 3 Dodeca cell (Bio-Rad) at the constant current of 15 mA per gel. The gels were then washed in the gel-fixing solution [10% (v/v) methanol, 7% (v/v) acetic acid] for 30 min and stained overnight with SYPRO Ruby protein gel stain (Bio-Rad). The gels were then rinsed in the fixing solution for 60 min and subsequently washed in water before imaging with a Pharos FX Plus Molecular Imager (Bio-Rad). The gels were further analysed using PDQuest software (Bio-Rad) and selected spots were identified by MS analysis (Department of Functional Genomics and Proteomics, FSc, MU).

**Table VII**: IEF conditions.

| Step No. | Function | Max. voltage | Voltage slope | Time |
|---|---|---|---|---|
| 1 | Desalting | 100 V | Rapid | Corresponding 100 Vh |
| 2 | Voltage increase | 250 V | Linear | Corresponding 250 Vh |
| 3 | Voltage increase | 1000 V | Linear | Corresponding 1000 Vh |
| 4 | Main focusing step | 4000 V | Rapid | Corresponding 45000 Vh |
| 5 | Final sustainment | 500 V | Rapid | 15 h |

## 7.      Mass spectrometric analyses

MS analyses were performed at the Department of Functional Genomics and Proteomics, FSc, MU. Protein spots selected for analysis were excised from 2-DE gels with an EXQuest Spot Cutter (Bio-Rad). After destaining, the proteins in the gel pieces were incubated with trypsin (sequencing grade, Promega) at 37°C for 2 h. The corresponding proteolytic digests were analysed with MALDI-MS/MS and LC-MS/MS.

MALDI-MS and MS/MS analyses were performed on an Ultraflex III mass spectrometer (Bruker Daltonik, Bremen, Germany) using a CHCA matrix in combination with an AnchorChip target. LC-MS/MS analysis was performed online using an EASY-nLC system (Proxeon) coupled with an HCTultra PTM Discovery System ion trap mass spectrometer equipped with a nanospray (Bruker Daltonik). LC separation was accomplished on a reverse-phase column with a water/acetonitrile gradient. The MASCOT 2.2 (MatrixScience, London, UK) search engine was used for processing the MS and MS/MS data. Database searches were done against the NCBI protein database and EMBL EST plant database.

## 8.      Transcription levels of defense genes

The expression of genes in leaf tissues was analysed by real-time quantitative PCR (RT-qPCR), using the fluorescent intercalating dye SYBR-Green, in a Light Cycler 480 (Roche). Total RNA was isolated from 100 mg of leaf tissue using TRI reagent (Ambion) and purified using the TURBO DNA-free kit (Ambion). Reverse transcriptase reactions were performed with the ImProm-II Reverse Transcription System (Promega), with 0.4 µg of total RNA in a volume of 20 µl, according to the manufacturer's instructions. cDNA was amplified by qPCR using gene-specific primers (see Table VIII) and GoTaq qPCR Master Mix (Promega) according to the manufacturer's instructions.  PCR amplification was carried out as follows: 45 cycles of DNA denaturation at 95 °C for 20 s, annealing and extension at 60 °C for 40 s, with three replicates for each analysed sample. The transcript level of each gene was normalized to that of elongation factor 1α (EF-1α to facilitate the quantification of gene expression relative to an endogenous control by the $\Delta\Delta C_T$ method.

**Table VIII:** RT-Q-PCR primers sequences.

| Gene | Primer sequence (5′ → 3′) |
|------|---------------------------|
| *GeLiP* | F*: GTC CAA GAT TTC TGC GTC GC |
|  | R*: TTT CCA GCT GCA CTA AGC CC |
| *GLN2* | F*: TCT GTG TAT GCT GCC CTC GAG |
|  | R*: CCA GGC TTT CTT GGG CTA CC |
| *NtPRp27* | F*: ATT GTA CCA CGA GAG CAC CCA |
|  | R*: GGT TTC ACC CAG TGG CTA GGT |
| *PR2Q* | F*: TCC AGC AGA TGT TGT GTC GCT |
|  | R*: GGC TTG GCT AGC AGC AAC ATT |
| *PR3Q* | F*: TCT GGA TCA CCA ATG GCA TT |
|  | R*: AGA AGC CAT GGC AGG ACA T |
| *PR5* | F*: CCG AGG TAA TTG TGA GAC TGG AG |
|  | R*: CCT GAT GGG TTG ATT AA GTG CA |
| *TuReP* | F*: TCA CCT GCG AAC CCT AAC GA |
|  | R*: CAC GCC CTG GAT TTC CTT CT |
| *EF-1α* | F*: TGT GAT GTT TTT GTT CGG TCT TTA A |
|  | R*: TCA AAA GAA AAT GCA GAC AGA CTC A |

\* F is the forward primer and R is the reverse primer, respectively.

## 9. <u>Chlorogenic acid analysis</u>

Chlorogenic acid, an intracellular marker of plant cells, was analyzed in both apoplastic fluid isolates and leave extracts to estimate the extent of intracellular contamination in apoplastic fluid isolates. Apoplastic fluid isolates were prepared as described above, when weight of leaves used for the isolation was about 32.0 g. Leaves extracts were prepared from 150 mg of plant tissue, which was added to 1 ml of 33% (v/v) acetone in water and disintegrated in a grinding mortar with sea sand. The content of the mortar was then pipeted in a microtube and extraction was carried out with ultrasound treatment (100 W, 15 min). After centrifugation (10 min, 13.000 x *g*), the supernatant was transferred into a sample vial for HPLC analysis.

For HPLC analysis a Hewlett Packard HP 1100 series instrument with a binary pump, a vacuum degasser, an autosampler, a thermostated column compartment, and a diode array detector was used. The column used was a reversed-phase Supelcosil LC-18-DB (Supelco). The solvents were (A) 0.25% (v/v) $H_3PO_4$ in water and (B) acetonitrile. The elution system was as follows: 0-5 min, 0-5% of B; 5-15 min, 5-15% of B; 15-20 min, 15-20% of B; 20-21 min, 20-60% of B. The flow rate was 1 ml.min$^{-1}$, the injection volume was 50 μl, and the column oven was set to 24 °C. The signal was monitored at 254 and 320 nm. For quantification purposes a calibration curve was made.

## 10.   <u>Capsidiol analysis</u>

Phytoalexin capsidiol content was analysed by HPLC two days after treatment with 250 nM elicitins, results of three independent analyses of each sample were averaged. The leave extracts that were prepared from 150 mg of plant tissue, which was added to 1 ml of 40% (v/v) aqueous MeOH, containing 0.5% (v/v) acetic acid, and disintegrated in a grinding mortar with sea sand. The content of the mortar was then pipeted in a microtube and extraction was carried out with ultrasound treatment (100 W, 15 min). After centrifugation (10 min, 13.000 x *g*), the supernatant was transferred into a sample vial for HPLC analysis.

For HPLC analysis a Hewlett Packard HP 1100 series instrument was used. The column used was a reversed-phase Supelcosil LC-8-DB (Supelco). The solvents were (A) MeOH and (B) $H_2O$. The elution system was as follows: 0-16 min, 30-20% of B; 16-20 min, 0% of B. The flow rate was 1 ml.min$^{-1}$, the injection volume was 40 μl, and the column oven was set to 24 °C. The signal was monitored at 210 and 254 nm. For quantification purposes, a calibration curve was made.

## 11.   <u>Fluorescence spectrometry</u>

Fluorescence spectrometry was performed on a Perkin Elmer Luminiscence Spectrometer LS 50B in a stirred cuvette. The sterol and phospholipid binding of proteins was measured according to previously described methods (*64, 69*) by the titration of proteins with DHE and NBD-PC in 10 mM MES (pH 7.0). Dissociation constants, $K_d$, of the lipid-protein complexes were determined by linear plots of *$1/C_b$* vs *$1/C_f$* using the equation *$1/C_b = (K_d/A)(1/C_f) + 1/A$*, where $C_b$, $C_f$, and *A* are the concentrations of bound lipid and free lipid, and the maximal binding capacity, respectively. The concentration of the bound lipid, $C_b$, was calculated as described previously (*8*). The excitation and emission wavelengths were 325 nm and 370 nm for DHE and 460 nm and 534 nm for NBD-PC. The values were read after equilibration.

## 12.   <u>Sterol exchange assay</u>

Sterol exchange assay was performed by Bc. Michal Obořil. Elicitin-induced sterol exchanges were measured using stigmasterol or cholesterol micelles (3 μM) added to 2 ml measuring buffer (10 mM MES pH 7.0), containing DHE micelles (0.63 μM) (*58*). DHE fluorescence was then

recorded in both the absence (to determine spontaneous transfer rates) and presence of the elicitins.

### 13.  Phospholipid exchange assay

Phospholipid exchange assay was also performed by Bc. Michal Obořil. Unilamellar vesicles were prepared as follows: donor vesicles contained NBD-labelled phosphatidylcholine (PC), phosphatidylserine (PS), and cholesterol; acceptor vesicles contained PC, PS, and cholesterol. Phospholipids and sterols were dissolved in chloroform and for each assay 0.32 mg NBD-PC or PC, 0.08 mg PS and 0.16 mg cholesterol were mixed, the chloroform was evaporated under nitrogen and traces of solvent were vacuum evaporated for 1 h. Then, 2 ml of measuring buffer (10 mM MES pH 7.0) was added, the mixture was vortexed under nitrogen and sonicated for three 5 min periods at 40 °C. Measurements of elicitin-induced PC exchanges were performed using NBD-PC/PS donor vesicles (1.5 μM NBD-PC) added to 2 ml measuring buffer (10 mM MES pH 7.0), containing PC/PS acceptor vesicles (3 μM PC). Fluorescence of NBD-PC was then recorded in the absence (spontaneous transfer) or the presence of elicitins.

### 14.  Synthesis of reactive oxygen species

The synthesis of reactive oxygen species (ROS) induced by cryptogein in tobacco cell cultures was measured by Mgr. Nikola Ptáčková using a luminometric method in an elicitation buffer. The concentrations of $H_2O_2$ were monitored every 10 min in 250 μl aliquots (*70*).

### 15.  Resistance analysis

The resistance analysis experiments were also performed by Mgr. Nikola Ptáčková. Systemic acquired resistance (SAR) was induced by elicitin application (*71*): plants were decapitated and their stems treated with 20 μl of water or a 5 μM aqueous solution of cryptogein. Inoculations with *Phytophthora parasitica* were performed by infiltrating leaf parenchyma tissue with a 50 μl suspension containing 100 zoospores (*72*). In each experiment, at least four consecutive leaves received two infiltrations of zoospore suspension each. Susceptibility and resistance were evaluated by measuring the areas over which disease symptoms were observed, at various numbers of days after inoculation, for each leaf. The development of disease symptoms is strictly correlated with the development of the oomycete (*73*).

All experiments were performed at least three times with three replicates of plants. Results are presented as mean ± standard deviation. A paired t-test was used to analyse differences between two groups.

## *Results*

Here I would like to highlight that the results presented in chapters Sterol and phospholipid transfer, Resistance to *Phytophthora parasitica*, and Induction of early events by mutated cryptogeins in tobacco cells suspension do not come from my personal work, but they were acquired by my coworkers, whose names are indicated in particular chapters. These results are shown in this thesis to further support conclusions in the Discussion section. All the other results come entirely from my own work.

## 1.     **Recombinant proteins production**

Dobeš and co-workers used computer modelling and quantitative structure-activity relationship analysis to design cryptogein variants with altered binding of lipid compounds (*7*). Construction and biochemical characterization of these mutants should provide insight into the role of lipid binding over the course of a defense reaction. We have prepared three recombinant cryptogeins carrying the following mutations: Leu41Phe (L41F), Val84Phe (V84F), and both Leu41Phe and Val84Phe (L41F/V84F). The mutated residues targeted a hydrophobic cavity of the elicitins. The proteins were produced using the eukaryotic *P. pastoris* expression system, to ensure that they retained their native folded structures. To promote the correct cleavage of α-secretion factor by *P. pastoris* proteases, a glycine residue was added to the N-terminus of the proteins. Using MALDI-MS analysis, the molecular weights (MW) of the generated proteins were found to be 10 386 Da for cryptogein, 10 418 Da for the L41F mutant, 10 433 Da for the V84F mutant, and 10 467 Da for the L41F/V84F double mutant. The measured molecular weights of the mutants relative to that of cryptogein are the same as the theoretical ones. The absolute molecular weights of all four proteins differ by 6 Da from the theoretical ones, which corresponds to three disulphide bridges. MS spectra are shown in Figure 7.
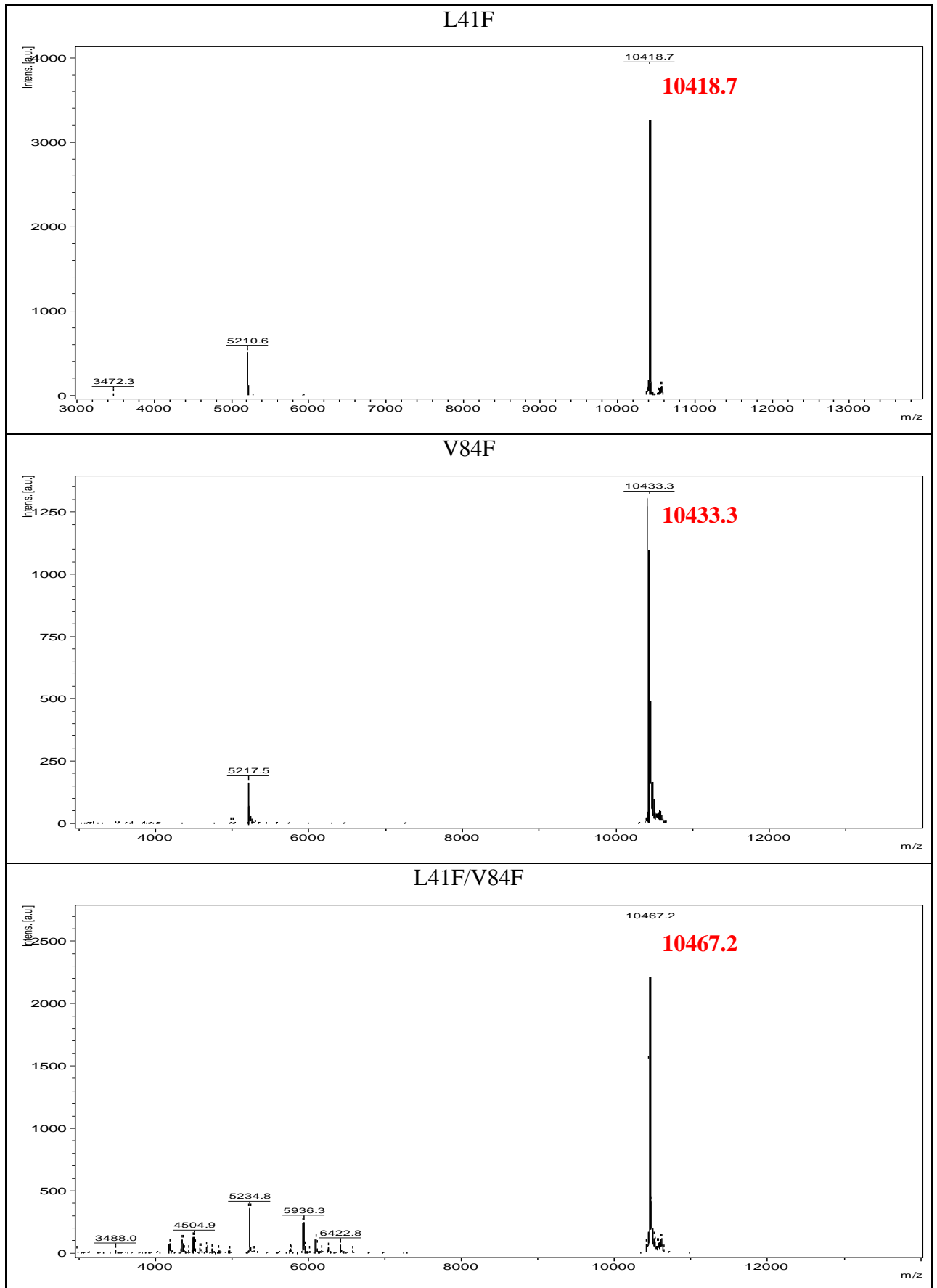
**Figure 7:** MS spectra of produced cryptogein mutants.

## 2. Sterol-binding activities and affinities

Elicitins have a hydrophobic core that can accommodate sterols or phospholipids. The sterol-binding activity of the wild type (wt) cryptogein and the L41F, V84F, and L41F/V84F mutants was determined using the fluorescent sterol dehydroergosterol (DHE). To exclude possible effects of non-specific binding, aprotinin was included as a negative control in all binding experiments since it has very similar properties to cryptogein (MW= 6.5 kDa, pI=10.1). Addition of aprotinin did not affect the DHE fluorescence in the assays.

Dissociation constants of the lipid-protein complexes were determined by linear plots of $1/C_b$ vs $1/C_f$ (see Figure 9) using the equation $1/C_b = (K_d/A)(1/C_f) + 1/A$, where $C_b$, $C_f$, and $A$ are concentrations of bound lipid, free lipid, and maximal binding capacity, respectively. For all measured proteins the number of binding sites was found to be approximately one per molecule. The determined values of $K_d$ are shown in Table IX, and are consistent with the predicted effects of the individual mutations. The calculated $K_d$ for the DHE-wt cryptogein complex corresponds to those estimated in previous studies (*8, 64*). The fluorescence binding curves are shown in Figure 8.
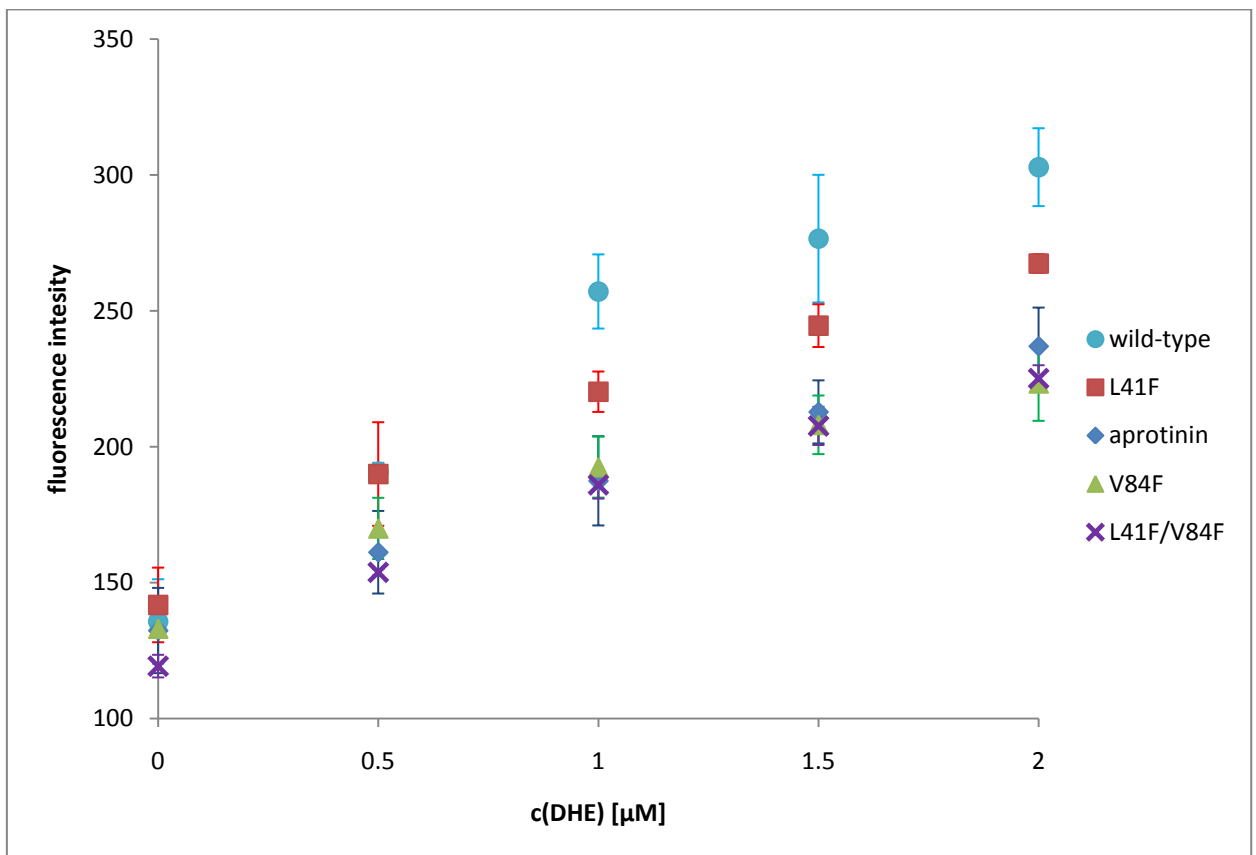


**Figure 8:** Fluorescence titration curves of mutated cryptogeins with DHE. 1 μM proteins were titrated in elicitation buffer with 0.5-2 μM DHE and the resulting fluorescence was read.
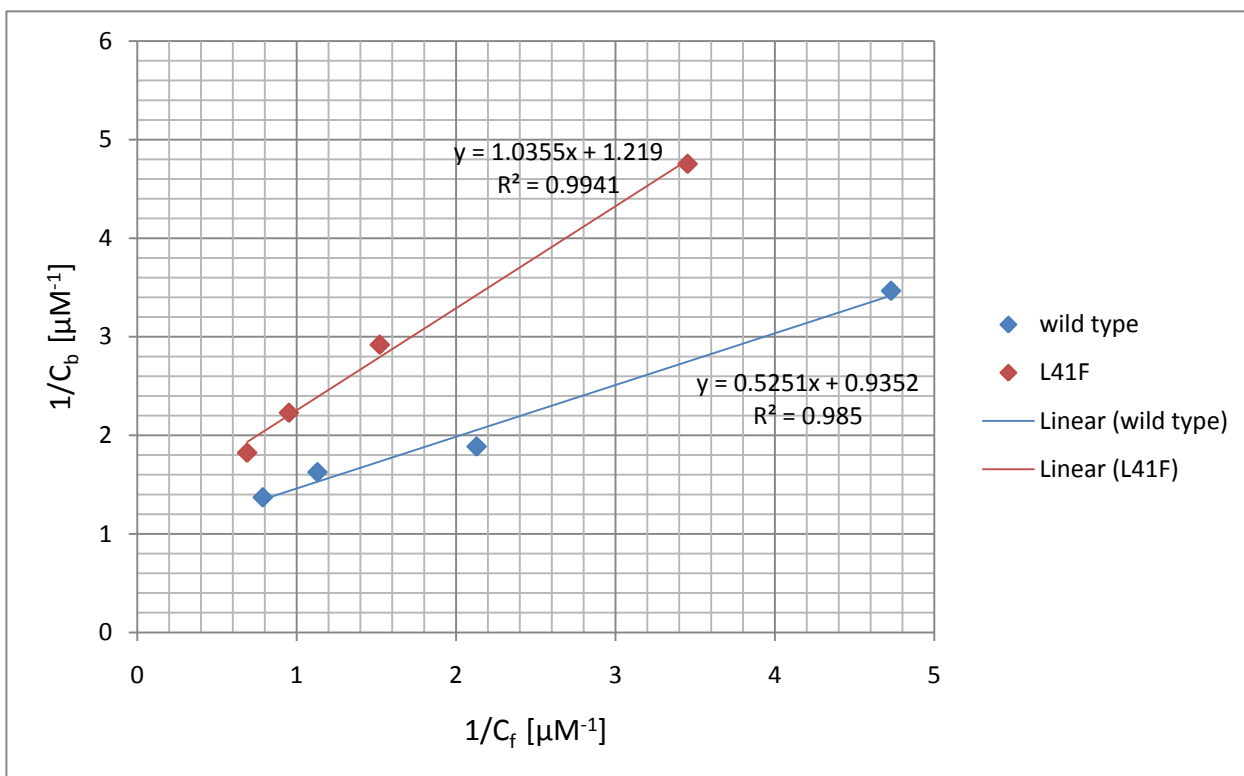
**Figure 7:** Linear plots of $1/C_b$ vs $1/C_f$. $C_b$ and $C_f$ are concentrations of bound lipid and free lipid, respectively.

## 3. Sterol and phospholipid transfer

From a physiological point of view an important feature of elicitins is their ability to interact with the plasma membrane and transfer sterols and phospholipids. In the present study, we used sterol micelles and DHE to evaluate the ability of the elicitins to transfer sterols between membranes (performed by Bc. Michal Obořil). The addition of the wt cryptogein stimulated a rapid increase in fluorescence; with a plateau after about 5 min owing to dilution of DHE in the stigmasterol micelles. The initial rates of fluorescence for the wt cryptogein and the mutants are given in Table IX. As expected, cryptogeins containing the V84F mutation showed a significantly reduced ability to transfer DHE between the membranes compared to the wt cryptogein. In the L41F mutant there was only a minor decrease in DHE transfer rate.

The transfer of phospholipids between the membranes was evaluated using a method based on the exchange of the fluorescently labelled phospholipid NBD-PC from unilamellar donor vesicles to PC acceptor vesicles as described above. Individual rates of fluorescence after addition of the elicitins are given in Table IX. Surprisingly, the V84F mutant and the double mutant showed higher rates of PC transfer than cryptogein. On the other hand, and consistent with expectations, the L41F mutant showed a lower rate of PC transfer.

To exclude the possibility that the observed transport was due to non-specific transport by the elicitins, aprotinin was used as a control. It did not elicit transport of sterols or phospholipids between the membranes (Table IX).

**Table IX**: DHE binding and lipid transfer activities of studied proteins.

| Protein | $K_d$ [µM] | DHE transfer | NBD-PC transfer |
|---|---|---|---|
| **Wild type** | 0.56 ± 0.04 | 2.51 ± 0.06 | 0.51 ± 0.05 |
| **L41F** | 0.85 ± 0.05 | 1.88 ± 0.08 | 0.32 ± 0.01 |
| **V84F** | No binding | 0.45 ± 0.02 | 0.74 ± 0.08 |
| **L41F/V84F** | No binding | 0.38 ± 0.01 | 0.76 ± 0.04 |
| **Aprotinin** | No binding | 0.19 ± 0.01 | 0.15 ± 0.01 |

Dissociation constants, $K_d$, of analysed proteins for DHE binding and initial rates of sterol (DHE) and phospholipid (PC) transfer measured by changes in DHE and NBD-PC fluorescence.

## 4. Induction of early events by mutated cryptogeins in tobacco cells suspension

We measured the effects of the mutations on the elicitation of the synthesis of reactive oxygen species (ROS) in tobacco cells in suspension (performed by Mgr. Nikola Ptáčková). Suspension cultures enable the exact parallel evaluation of the early events over time. The tobacco cell suspensions were elicited with 50 nM cryptogein solutions. The levels of hydrogen peroxide over time are shown in Figure 10B. The double mutant L41F/V84F stimulated almost no synthesis of ROS. On the other hand, although the V84F mutant was unable to bind DHE (Table IX), it was almost as efficient as the wt cryptogein in stimulating ROS synthesis. The production of ROS stimulated by the L41F mutant, which showed a lower ability to transfer PC, was about half that of the wt cryptogein, with the maximum shifted to 10 min.

## 5. Accumulation of capsidiol

Capsidiol production is triggered either by pathogen attack or by biotic and abiotic elicitors; it acts as an anti-microbial compound against pathogens. From tobacco leaves, extracts for a reverse-phase HPLC based capsidiol analysis were prepared as described above. The results of the analysis are shown in Figure 10C. The L41F mutant and L41F/V84F double mutant (DM) showed a very low ability to trigger capsidiol synthesis, which correlates well with reductions in their ROS accumulation and necrotic effects.
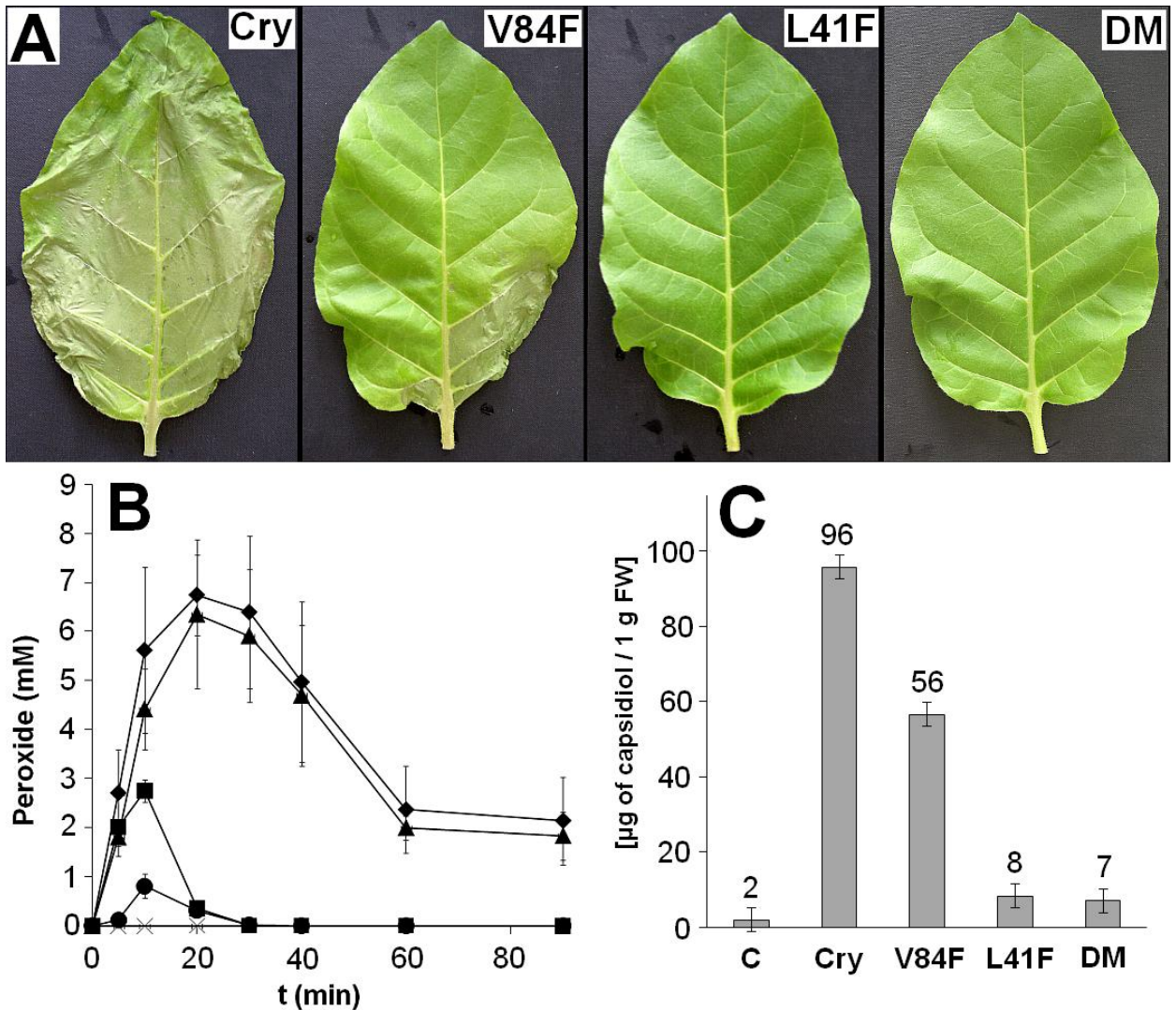
**Figure 10:** Extent of hypersensitive response (HR), ROS production and capsidiol content after application of individual elicitins. (A) Leaves with the most extensive HR 3 days after treatment with 250 nM elicitins. (B) ROS synthesis in tobacco cells in suspension stimulated by elicitins – wild type cryptogein (diamonds), V84F (filled triangles), L41F (squares), L41F/V84F (circles) and control (X). Cells were equilibrated for 3 h in an elicitation buffer, and elicitins were added to the suspension at time zero. The concentrations of $H_2O_2$ were monitored every 10 min in 250 μl aliquots by a luminol method. (C) Capsidiol content analysed by HPLC analysis 2 days after treatment with 250 nM elicitins, results for three independent analyses of each sample were averaged. Cry = wild type cryptogein, DM = L41F/V84F double mutant, C = control (leaves treated with water).

**Figure 8**: HPLC chromatogram from capsidiol analysis. The red arrow signs the capsidiol peak. Samples - extract from leaves treated with wild-type cryptogein is shown by an unbroken line, extract from leaves treated with water is shown by a dashed line.



**Figure 9**: HPLC chromatogram from capsidiol analysis. The red arrow signs the capsidiol peak. Samples - extract from leaves treated with wild-type cryptogein is shown by an unbroken line, extract from leaves treated with L41F/V84F cryptogein mutant is shown by a dashed line.

## 6.     <u>Proteomic analysis</u>

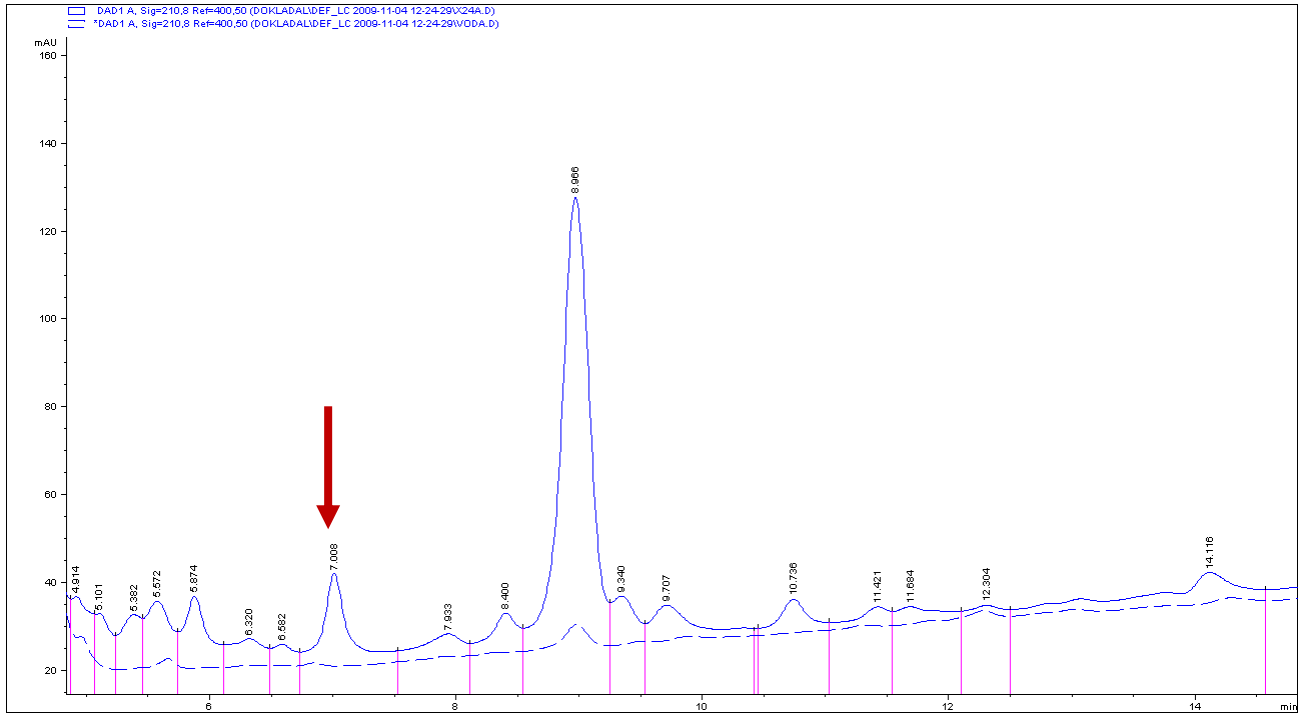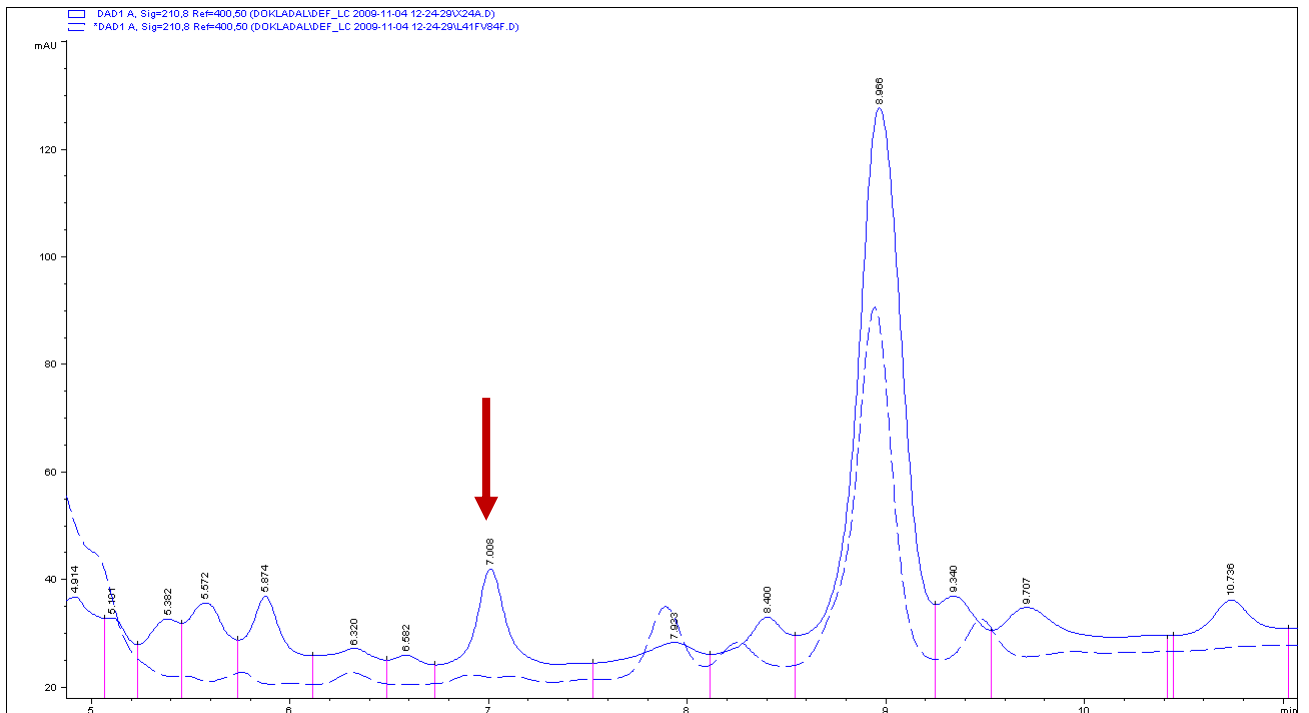To study the effect of the four cryptogeins on the expression of proteins involved in defense response, an analysis of intercellular fluid (IF) was conducted. The main reason for analysis of IF was that the majority of secreted pathogenesis-related proteins are expressed into intercellular space. Tobacco leaves were treated by soaking the petioles in 250 nM aqueous solutions of the cryptogeins for 48 hours. Leaves treated with water were used as a control. Varying levels of hypersensitive response, up to one third of the leaf area, were observed for the different proteins (Figure 10A). The L41F mutant and the L41F/V84F double mutant (DM) induced almost no necrotic symptoms and the V84F mutant induced a lower extent of hypersensitive response than the wt cryptogein.

The proteomic experiment was designed so that a good compromise between plant and other material consumption and separation quality could be obtained. To minimize protein losses during sample preparation for IEF, the precipitation step was omitted. For a triplicative 2-D separation of one sample, isolates from 15 leaves were used, namely upper, middle and lower leaves from each of five plants. Moreover, chlorogenic acid, an intracellular marker of plant cells, was analysed in both apoplastic fluid isolates and leaf extracts to estimate the extent of intracellular contamination in apoplastic fluid isolates. Samples with standard addition were used to identify the chlorogenic acid peak position. The peak absorption spectrum is shown in Figure 14 and corresponds to the UV absorption spectrogram of chlorogenic acid published previously (*74*). An example of a related chromatogram is shown in Figure 13. The calculated contaminations are shown in Table X and it is obvious that no sample was significantly contaminated with intracellular content.

After the isolation step, 2-D electrophoresis of tobacco extracellular proteins with subsequent MS identification (MALDI-MS and LC-MSMS) of spots selected on the basis of PDQuest analysis was performed (Figure 15). We focused on qualitative changes; spots were selected according to their unique occurrence in particular samples. Owing to the low overall concentration of the proteins isolated from the intercellular fluid, gel-staining using a highly sensitive fluorescent stain, SYPRO Ruby (Bio-Rad), was used.

After treatment of tobacco leaves with the cryptogeins, a massive induction of protein expression into tobacco intercellular space occurred (for spot counts from the PDQuest analysis see Table X). The highest induction was observed for the V84F mutant whilst the lowest was found for the double mutant. The highest correspondence in counted spots was found for the wt cryptogein and the V84F mutant and, as expected, the lowest was found for the control and the wt cryptogein

(Table X). Subsequent MS identification of selected spots proved that the majority of the identified proteins play a role in plant-pathogen interactions and are naturally located extracellularly. The results of MS analysis are shown in Table XI; for mascot score and coverage see Table XII. Surprisingly, the results do not show a strong correlation between the ability of an elicitin to bind or transfer sterols or phospholipids and the level of expression of extracellular proteins with defense response roles. Similarly, although the L41F mutation does not significantly alter the sterol and phospholipid transfer rates, it has a strong influence on the expression of defense proteins. The role of the identified proteins in plant-pathogen interaction and the dependence of their expression on elicitin design are considered further in the discussion section.

**Table X:** Spot counts from the proteomic analysis of individual proteins and intracellular contamination.

| Elicitin | Intracel. cont. | Spot count | | Count of common spots | | | |
|---|---|---|---|---|---|---|---|
| | | **Total** | **Unique** | **Cryptogein** | **V84F** | **L41F** | **L41F/V84F** |
| Cryptogein | 6.4 % | 144 | 26 | - | 94 | 44 | 27 |
| V84F | 7.4 % | 171 | 36 | 94 | - | 56 | 23 |
| L41F | 2.3 % | 137 | 38 | 44 | 56 | - | 29 |
| L41F/V84F | 5.6 % | 71 | 16 | 27 | 23 | 29 | - |
| Control | 5.7 % | 23 | 2 | 9 | 8 | 14 | 21 |

The gels were analysed using PDQuest software (Bio-Rad). Contamination of apoplastic fluid (Intracel. cont.) with intracellular content was calculated on the base of chlorogenic acid content in both apoplastic fluid and leaf extracts.
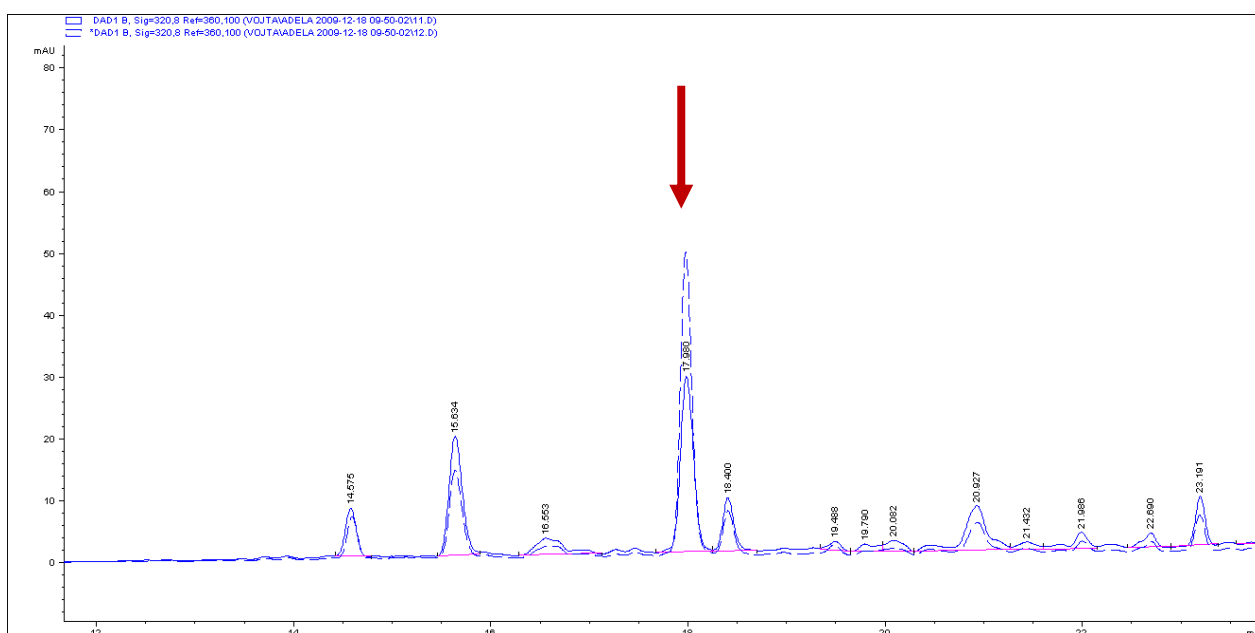


**Figure 13**: HPLC chromatogram from chlorogenic acid analysis. The red arrow signs the chlorogenic acid peak. A sample with an internal standard of chlorogenic acid is shown by the dashed line. The unbroken line shows the same sample without the internal standard of chlorogenic acid.
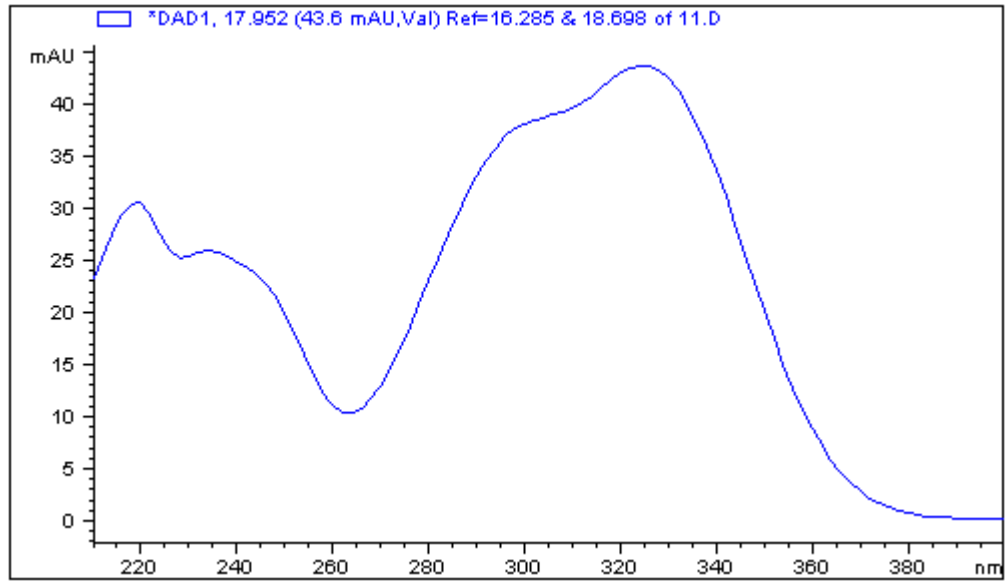
**Figure 14:** UV absorption spectrum of chlorogenic acid.
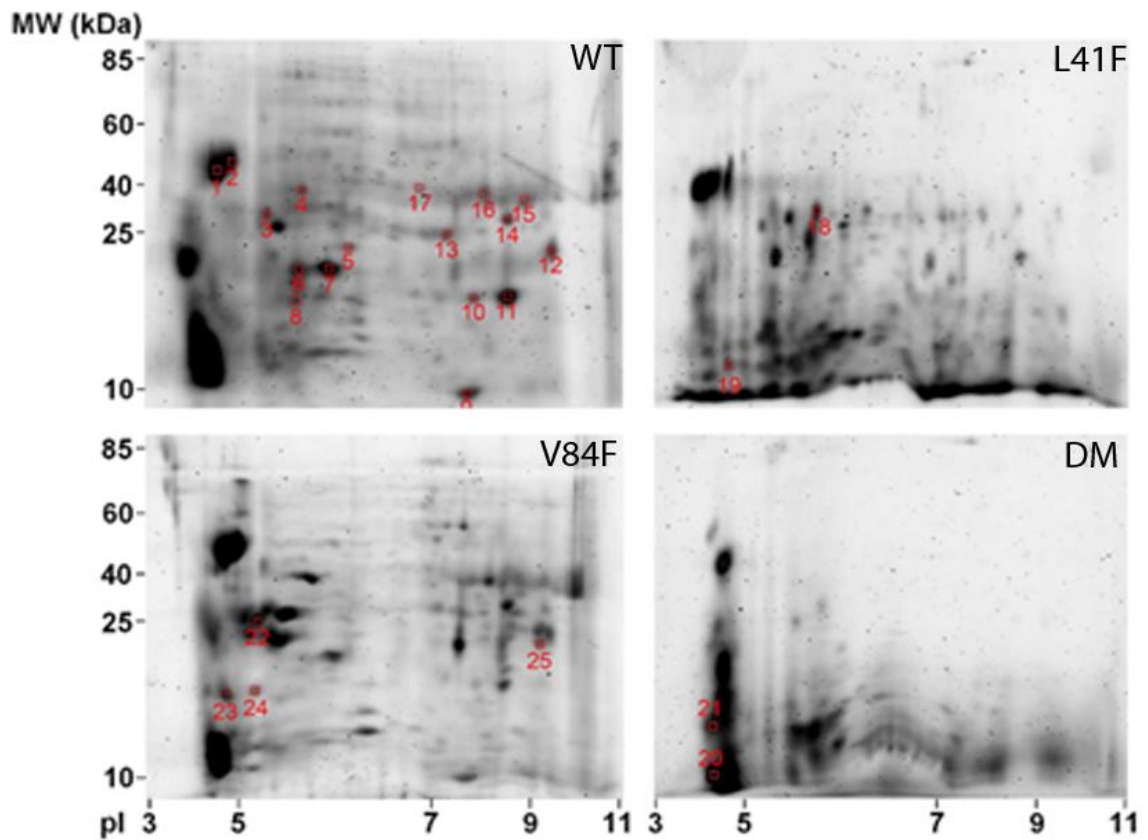


**Figure 15:** 2D gel electrophoresis proteome maps of intercellular fluid determined 48 hours after application of cryptogein and its mutants. Identified proteins with qualitative changes between individual samples are indicated. For the first dimension of separation, 80 µg of protein was applied to each IPG strip (7 cm, pH 3–10 NL). For separation in the second dimension, 12% SDS–PAGE was carried out. Proteins were visualized by SYPRO Ruby staining. Isoelectric points (pI) and molecular weights (MW, kDa) are marked. WT = wild type cryptogein, DM = L41F/V84F double mutant.

**Table XI:** Identified proteins.

| Protein | NCBI accession No. | Spot No. | MM [kDa] | pI | Cry | L41F | L41F/ V84F | V84F |
|---|---|---|---|---|---|---|---|---|
| **β-1,3-glucanases** | | | | | | | | |
| Glucan endo-1,3-β-glucosidase | 19859 | 4 | 37.8 | 5.2 | + | | | + |
| Glucan endo-1,3-β-glucosidase | 19869 | 13, 14, 15 | 40.4 | 7.1 | + | | | + |
| **Chitinases** | | | | | | | | |
| CBP20 | 632736 | 8, 12, 17 | 21.9 | 8.4 | + | + | + | + |
| PR-4A | 19962 | 8 | 16.2 | 7.6 | + | | + | + |
| PR-4B | 100352 | 19, 21 | 15.2 | 6.1 | + | + | + | + |
| Endochitinase A | 116314 | 14, 15 | 35.1 | 8.4 | + | | | + |
| Endochitinase B | 116321 | 16 | 34.7 | 8.3 | + | | | + |
| Acidic chitinase PR-P | 19771 | 22, 24 | 27.5 | 4.9 | + | + | | + |
| Acidic chitinase PR-Q | 19773 | 3, 18 | 27.6 | 5.1 | + | + | | + |
| NtChitIV chitinase | 121663827 | 23, 5 | 29.9 | 4.9 | + | | | + |
| Chi-5 (Chitinase/lysozyme) | 467689 | 12 | 42.0 | 9.1 | + | | | + |
| **Proteinase inhibitors** | | | | | | | | |
| Proteinase inhibitor I-A | 547732 | 9 | 11.9 | 7.8 | + | | | + |
| Proteinase inhibitor I-B | 547733 | 9 | 11.9 | 7.8 | + | | | + |
| **Peroxidases** | | | | | | | | |
| Lignin-forming anionic peroxidase | 129837 | 1, 2, 20, 21 | 34.7 | 4.7 | + | + | + | + |
| Peroxidase | 63002585 | 15 | 35.6 | 8.4 | + | | | + |
| **Peptidyl-prolyl isomerases** | | | | | | | | |
| Cyclophilin-like protein | 152206078 | 11 | 22.0 | 7.8 | + | | | + |
| Peptidyl-prolyl isomerase, putative [*Ricinus communis*] | 255547634 | 10, 11 | 27.5 | 9.6 | + | | | + |
| **Other** | | | | | | | | |
| Germin-like protein | 222051768 | 6 | 21.4 | 5.8 | + | | + | + |
| NtPRp27 | 5360263 | 25 | 27.4 | 9.3 | + | | | + |
| Thaumatin-like protein E22 | 131015 | 22 | 24.7 | 5.4 | + | + | | + |
| Tumor-related protein | 1762933 | 7 | 23.4 | 8.5 | + | | | + |

Differentially expressed proteins identified by MALDI-TOF-MS and/or LC-MS/MS analysis of tryptic peptides followed by searches against the NCBI database (non redundant, all entries) and EST-Plants protein database in each protein, showing their individual spot numbers and presence (+). The corresponding NCBI accession numbers, the theoretical molecular mass (MM) and pI values are also indicated. The scores and percentages of protein coverage (% Cov) for both MALDI-MS and LC-MS/MS are listed in Table XII.

**Table XII:** The scores and percentages of protein coverage (% Cov) for both MALDI-MS and LC-MS/MS.

| Protein name | NCBI accession No. | MW [kDa] | pI | Spot No. | MALDI-MS Score | MALDI-MS % Cov | LC-MSMS Score | LC-MSMS % Cov | In samples |
|---|---|---|---|---|---|---|---|---|---|
| Acidic chitinase PR-P | 19771 | 27.5 | 4.9 | 22 | 660 | 50 | 164 | 15 | WT, V84F |
|  |  |  |  | 24 | 277 | 12 | 136 | 5 | L41F, V84F |
| Acidic chitinase PR-Q | 19773 | 27.6 | 5.1 | 3 | - | - | 46 | 8 | WT, V84F |
|  |  |  |  | 18 | - | - | 50 | 3 | L41F |
| CBP20 | 632736 | 21.9 | 8.4 | 8 | - | - | 117 | 9 | WT, L41F/V84F, V84F |
|  |  |  |  | 12 | - | - | 126 | 9 | WT, V84F |
|  |  |  |  | 17 | - | - | 117 | 9 | WT, L41F/V84F, V84F |
| Class IV chitinase | 121663827 | 29.9 | 4.9 | 23 | - | - | 103 | 22 | V84F |
|  |  |  |  | 5 | - | - | 51 | 7 | WT, V84F |
| Chitinase/lysozyme | 467689 | 42.0 | 9.1 | 12 | - | - | 116 | 3 | WT, V84F |
| Cyclophilin-like protein | 152206078 | 22.0 | 7.8 | 11 | - | - | 64 | 13 | WT, V84F |
| Endochitinase A | 116314 | 35.1 | 8.4 | 14 | - | - | 68 | 4 | WT, V84F |
|  |  |  |  | 15 | - | - | 68 | 7 | WT, V84F |
| Endochitinase B | 116321 | 34.7 | 8.3 | 16 | - | - | 69 | 8 | WT, V84F |
| Germin like protein | 222051768 | 21.4 | 5.8 | 6 | - | - | 59 | 8 | WT, L41F/V84F, V84F |
| Glucan endo-1,3-β-glucosidase | 19859 | 37.8 | 5.2 | 4 | 176 | 14 | 259 | 24 | WT, V84F |
| Glucan endo-1,3-β-glucosidase | 19869 | 40.4 | 7.1 | 13 | - | - | 98 | 3 | WT, V84F |
|  |  |  |  | 14 | 224 | 14 | 182 | 18 | WT, V84F |
|  |  |  |  | 15 | 272 | 18 | 118 | 15 | WT, V84F |
| Proteinase inhibitor I-A | 547732 | 11.9 | 7.8 | 9 | 57 | 16 | - | - | WT, V84F |
| Proteinase inhibitor I-B | 547733 | 11.9 | 7.8 | 9 | 191 | 15 | - | - | WT, V84F |
| Lignin-forming anionic peroxidase | 129837 | 34.7 | 4.7 | 1 | 245 | 11 | 159 | 20 | WT, V84F |
|  |  |  |  | 2 | 419 | 20 | 134 | 20 | WT, V84F |
|  |  |  |  | 20 | 143 | 5 | - | - | L41F/V84F |
|  |  |  |  | 21 | 266 | 11 | 148 | 10 | L41F, L41F/V84F |
| NtPRp27 | 5360263 | 27.4 | 9.3 | 25 | 258 | 16 | 114 | 16 | WT, V84F |
| PR-4A | 19962 | 16.2 | 7.6 | 8 | - | - | 86 | 8 | WT, L41F/V84F, V84F |
| PR-4B | 100352 | 15.2 | 6.1 | 19 | - | - | 76 | 9 | L41F, V84F |
|  |  |  |  | 21 | - | - | 125 | 9 | L41F, L41F/V84F |
| Peptidyl-prolyl cis-trans isomerase, putative [Ricinus communis] | 255547634 | 27.5 | 9.6 | 10 | 192 | 12 | 92 | 12 | WT, V84F |
|  |  |  |  | 11 | 316 | 21 | - | - | WT, V84F |
| Peroxidase | 63002585 | 35.6 | 8.4 | 15 | - | - | 90 | 9 | WT, V84F |
| Thaumatin-like protein E22 | 131015 | 24.7 | 5.4 | 22 | - | - | 144 | 33 | WT, L41F, V84F |
| Tumor-related protein | 1762933 | 23.4 | 8.5 | 7 | 178 | 8 | - | - | WT, V84F |

Protein name, according to literature or NCBI database; NCBI accession No., number of protein in NCBI database; pI, theoretical pI; MW, theoretical molecular weight; Spot No., number of identified spot on 2-D gel; Score, Mascot score and amino acid sequence; % Cov, percentage of coverage of the identified proteins; In samples, samples in which given protein was found.

## 7.	Accumulation of defense gene transcripts

To investigate the relationship between the proteomic data and gene expression, the transcript level for selected proteins was evaluated with RT-qPCR assays. Based on the proteomic analysis the following genes were selected for transcript quantification: *PR2Q*, *PR3Q*, *PR5*, *GLN2*, *TuReP*, *NtPRp27*, and *GeLiP*. Transcript levels of all of these determined genes were related to those induced in the water sample used as a control. The results are summarized in Table XIII; correlations with the proteomic data can be seen. For the double mutant, we observe no or only a minimal increase in transcript levels, whereas for the V84F mutant, the increases in transcript levels are similar to or higher than those observed for the wt cryptogein.

**Table XIII:** Accumulation of defense-related genes.

| Gene | A.N. | Cryptogein | | V84F | | L41F | | L41F/V84F | |
|---|---|---|---|---|---|---|---|---|---|
| | | logR | SD | logR | SD | logR | SD | logR | SD |
| *PR2Q*<br>β-1,3-glucanase | X54456 | 1.04 | 0.12 | 1.32 | 0.12 | 0.80 | 0.09 | 0.03 | 0.12 |
| *GLN2*<br>β-1,3-glucanase | X53600 | 1.08 | 0.13 | 1.12 | 0.13 | 0.64 | 0.14 | -0.10 | 0.12 |
| *PR3Q*<br>Chitinase | X51425 | 1.02 | 0.15 | 1.00 | 0.11 | 0.57 | 0.12 | -0.07 | 0.10 |
| *PR5*<br>Thaumatin-like protein | X12739 | 1.23 | 0.19 | 1.76 | 0.11 | 1.04 | 0.07 | 0.35 | 0.10 |
| *TuReP*<br>Tumor-related protein | FG644925 | 2.35 | 0.13 | 1.83 | 0.04 | 0.68 | 0.15 | 0.28 | 0.07 |
| *NtPRp27* | FG633857 | 1.02 | 0.15 | 1.29 | 0.12 | 0.67 | 0.07 | 0.51 | 0.06 |
| *GeLiP*<br>Germin-like protein | AB449366 | 0.64 | 0.13 | 0.82 | 0.05 | n.d. | n.d. | 0.46 | 0.11 |

Effect of the the wild type cryptogein and the mutants L41F, L41F/V84F, and V84F on accumulation of transcripts for PR and other defense related proteins. Gene expression relative to a control was calculated by the ΔΔC(t) method. The values given in the table are the logarithm of the relative increase (logR) and its standard deviation (SD). More than a two-fold increase in gene expression was taken as significant. A.N. = accession number of gene in NCBI database.

## 8.	Resistance to *Phytophthora parasitica*

The results presented above, particularly from the proteomic analysis, suggest that introduction of the L41F mutation to cryptogein would reduce the level of resistance induced. To verify this, resistance of tobacco plants to the fungal pathogen *Phytophthora parasitica* was evaluated (by

Mgr. Nikola Ptáčková). As expected, there was no induction of resistance for plants treated with the L41F mutant or the L41F/V84F double mutant. The resistance induced by the V84F mutant was comparable to that of the wt cryptogein (Figure 16).
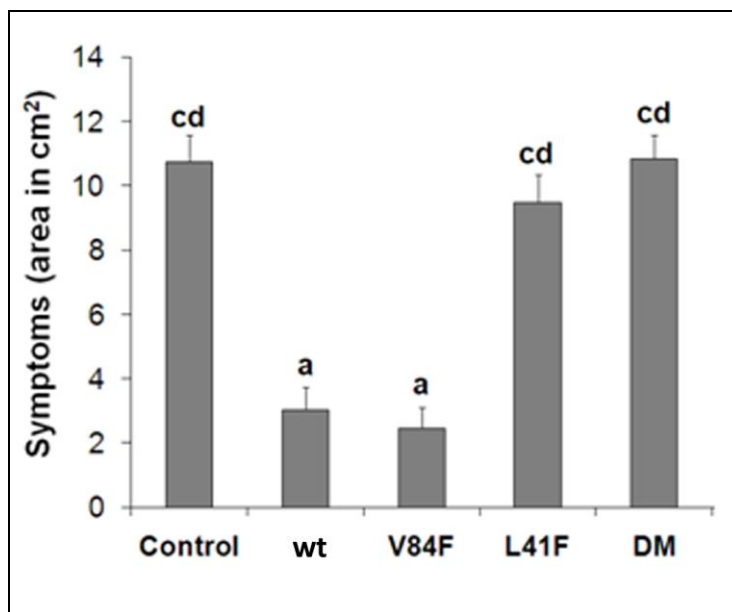


**Figure 16:** Induction of resistance against *Phytophthora parasitica* in tobacco plants. Leaves from 8 week old tobacco plants treated with elicitins were inoculated with zoospores of *P. parasitica*. The invaded areas were measured 3 days after inoculation. Each bar represents the standard error of four replicates from three different experiments. A replicate corresponds to eight inoculated areas on four leaves from one plant. Student's *t*-test with $p = 0.01$ was used to determine whether differences in area were statistically significant. Wt = wild type cryptogein, DM = L41F/V84F double mutant, Control = plants treated with water.

## *Discussion*

To clarify the relationship between the lipid-loading properties of elicitins and the course of the defense reaction we constructed three new cryptogein mutants: Leu41Phe (L41F), Val84Phe (V84F), and a double mutant Leu41Phe/Val84Phe (L41F/V84F), for which no structural changes were expected (*7*). Substitution of the amino acid residue Leu41 with a larger hydrophobic amino acid should decrease the binding of phospholipids in the cavity of cryptogein, while preserving the binding of sterols. Similarly, substitution of the residue Val84 with a large hydrophobic amino acid should reduce the binding of sterols in the cavity without affecting the binding of phospholipids.

Data from sterol (specifically, DHE) and phospholipid (specifically, PC) binding assays were in agreement with expectations based on the structural data of the DHE-cryptogein and PC-cryptogein complexes reported previously (*7*). The V84F and V84F/L41F mutants exhibited no measurable binding of DHE. For the L41F mutant, there was observed only a slight decrease in binding affinity for DHE compared to the wt cryptogein. Furthermore, using a simple fluorimetric method with donor and acceptor micelles we found that all mutants were able to transport DHE. However, in mutants carrying the V84F substitution there was approximately a 90% inhibition of the transfer rate compared only to a 27% inhibition for the L41F mutant. In the PC exchange experiments, approximately a 50% inhibition of transfer was observed for the L41F mutant, while for the mutants carrying the V84F substitution there was a higher rate of exchange than for the wt cryptogein. This unexpected finding can be explained by the fact that mutation of a small valine residue for a large phenylalanine residue could have resulted in a relaxing of the cavity groove, facilitating the binding of highly flexible phospholipids.

To test the effect of the mutations on the induction of early events in defense response, we measured the synthesis of ROS in tobacco cells in suspension when treated with the cryptogeins. A previous study suggested two signaling pathways for elicitin-induced responses and the necessity of a conformational change in the ω-loop, induced by sterol binding, to induce the early events (*8*). Contrary to this hypothesis, the V84F mutant, with a substantially lowered ability to bind and transfer sterols, was as efficient as the wt cryptogein in stimulating ROS production; and the L41F mutant, with only a slightly lowered ability to bind and transfer sterols, was far less efficient in inducing the synthesis of ROS (Figure 10B). The L41F/V84F double mutant showed almost no ability to transfer and bind sterols, and led to almost no ROS synthesis.

Structure-prediction of the Leu41Phe and Leu41Phe/Val84Phe mutants revealed that the large phenylalanines are easily accommodated by the surrounding residues without any significant changes in the ω-loop (*7*). The highly conserved structure of the ω-loop suggests it has an important biological function. We speculate that the mutation of a small leucine residue for a large hydrophobic phenylalanine residue could alter the interaction of the protein with the high affinity binding site on the plasma membrane. Detailed characterization of elicitin interaction with this high affinity binding site is ongoing in our laboratory.

We used proteomic analysis of intercellular fluid to study the overall changes induced by cryptogein and its mutants at the protein level. The proteomic experiment was designed so that a good compromise between plant and other material consumption and separation quality was found. For a triplicative 2-D separation of one sample, five tobacco plants and 375 μg of particular recombinant cryptogeins were used. To minimize protein losses during sample preparation for IEF, the precipitation step was omitted. The use of Mini-PROTEAN 3 Dodeca cell (Bio-Rad) also contributed to material saving while providing sufficient protein separation. Gel staining using a highly sensitive fluorescent stain SYPRO Ruby (Bio-Rad) was another factor minimizing material consumption.

Intercellular fluid was chosen because during the defense reaction the majority of proteins tightly connected with the defense response are secreted into it. Proteins in intercellular fluid form a first barrier to pathogen attack; most of them are involved in suppression of the pathogen spreading. The extent of hypersensitive response in leaves after elicitin application via the petioles correlated quite well with the level of ROS synthesis in suspension cultures and the level of capsidiol accumulation (Figure 10). The lower level of hypersensitive response observed for the V84F mutant compared to the wt could be the result of different effective elicitin concentrations in the leaves, which can lead to increased differences in the defense response, as noted previously (*8*). Treatment of tobacco leaves with the wt cryptogein and the mutants led to substantial qualitative changes in the intercellular fluid proteome (Figure 15). These changes were more prominent for the wt cryptogein and the V84F mutant. The majority of identified proteins are naturally located extracellularly (Table XI), which together with chlorogenic acid analysis results, with maximal intracellular contamination of 7.4 % (Table X), shows a good quality of apoplastic fluid isolation.

Two different β-1,3-glucanases (PR-2 family) were identified for the wt cryptogein and the V84F mutant but not for the other mutants (Table XI). This finding coincided with the mRNA expression analysis which showed that the L41F mutant induced increases in the transcript levels of *PR2Q*, but these increases were significantly lower than those induced by the wt cryptogein

and the V84F mutant (Table XIII). This observation is consistent with the finding that several types of β-1,3-glucanases with different substrate specificities and specific activities are constitutively present in plants and can be considerably enhanced by pathogen-infection or stress (*75, 76*). Glucanases identified in tobacco have been shown to suppress diseases caused by *Phytophtora spp.*, *Rhizoctonia solani* and *Cercospora nicotianae (77)*.

We identified nine proteins with a chitin-binding domain or chitinase activity (Table XI). Since chitinases hydrolyze internal β-1,4-glycosidic linkages of chitin, they are involved in the release of chitin oligosaccharide elicitors from fungal cell walls upon infection. The expression of two of these proteins, PR-4 family members PR-4B and CBP20, was induced by all four of the elicitins studied. Ponstein *et al.* (1994) concluded that the stress induction pattern of CBP20 matches the stress induction pattern of other class I PR-proteins and demonstrated that CBP20 exhibits antifungal activity toward *Trichoderma viride* and *Fusarium solani* by causing lysis of the germ tubes and/or growth inhibition (*78*). PR-4B belongs to the PR-4 protein subgroup II, based on the absence of a hevein domain, for which a ribonuclease activity has been recently proposed (*79, 80*). PR-4A was identified for all but the L41F mutant. All the other identified chitinases belong to the PR-3 family. Endochitinase A and B were detected only for cryptogein and the V84F mutant. These belong to class Ib and inhibit the growth of many fungi in vitro by causing lysis of hyphal tips (*81, 82*). The acidic chitinases PR-Q and PR-P were detected for all the elicitins analysed except the L41F/V84F double mutant. These belong to class II and, even though chitinases of class II are very homologous to those of class I, antifungal activity has not been shown (*82*). However, the combination of class I and II chitinases and class I β-1,3-glucanases synergistically inhibit fungal growth (*77*). Moreover, the level of *PR3Q* transcript accumulation correlates well with the proteomic data; the double mutant did not stimulate any increase in transcription of *PR3Q*. The remaining two chitinases were detected for cryptogein and the V84F mutant. These belong to class IV (NtChitIV) and class V (Chi-V). NtChitIV may have an important function in early general defense responses (*83*). Chi-V is homologous to bacterial exo-chitinases and synergistic antifungal activity with class I β-1,3-glucanase has been shown (*84*).

Lignin-forming anionic peroxidase was identified for all four elicitins (Table XI). This belongs to the PR-9 family, a specific set of peroxidases that may contribute to cell wall reinforcement by catalysing lignifications and thus enhance resistance against pathogens (*76*). Another identified peroxidase, of molecular weight 35.6 kDa and pI 8.4, was induced only in the wt cryptogein and V84F mutant samples. It shows a very high homology to a previously identified peroxidase due

to the gene *tpoxN1*, belonging to the class III of plant peroxidases induced by wounding. Tobacco peroxidase gene (*tpoxN1*) is induced locally after wounding and then systematically in tobacco plants when its expression is induced by spermine (*85*).

In addition to the β-1,3-glucanases, proteinase inhibitors, peptidyl-prolyl isomerases, NtPRp27, and tumor-related protein were identified only in the wt cryptogein and V84F samples (Table XI). This correlated quite well with the transcript analysis (Table XIII). Proteinase inhibitors, which are induced after wounding and TMV infection, may target nematodes and herbivorous insects (*86*). Cyclophilins, also known as peptidyl-prolyl *cis-trans* isomerases, catalyze *cis-trans* isomerization of imide bonds in peptides and proteins and may be implicated in protein folding and in long-range interaction between cells. For some cyclophilin-like proteins, antifungal and antiviral activities have been found (*87*). NtPRp27 (PR-17 family) has been shown to accumulate after TMV infection and mechanical wounding, as well as after drought and ABA treatments (*49*). Tumor-related protein is similar in amino acid sequence to Kunitz-type trypsin inhibitors and this, together with its specific induction after elicitor treatment, indicates its possible role in plant-pathogen interaction.

Germin-like protein was identified in the wt cryptogein, V84F and L41F/V84F samples and the results from the proteomic analysis (Table XI) correlate well with those from the transcript analysis (Table XIII). Germin-like proteins are targeted to the cell wall and apoplast and the mechanism by which they influence plant defense is likely to be related to their generation of reactive oxygen species (*88, 89*). The last identified protein, thaumatin-like protein E22, belongs to the PR-5 family, which has been associated with activity against oomycetes (*76*). This protein was not identified in the L41F or L41F/V84F samples, which agrees with the reduced expression of the corresponding gene (*PR5*, Table XIII).

Proteomic analysis revealed that the V84F mutation, in contrast to the L41F mutation, did not limit the induction of plant defense-related proteins (Table XI). Even though the mutants carrying the L41F mutation induced increases in the levels of some transcripts, these increases were significantly lower than those induced by the wt cryptogein and the V84F mutant (Table XIII). Moreover, the key role of the identified proteins in resistance induction to *Phytophtora parasitica* has been shown. Whilst the wt cryptogein and the V84F mutant induced comparable resistance, the L41F mutant induced only very weak resistance and the double mutant did not induce any resistance (Figure 16). These findings all correlate well with the results of capsidiol analysis (acting as an anti-microbial compound) and the ROS experiments on the cell suspensions and further support the hypothesis formulated above that the Leu41 residue is

important in the interaction of cryptogein with the high affinity binding site on the plasma membrane.

Our results suggest that sterol binding to the cavity and the associated conformational change in the ω-loop might not play a principal role in cryptogein's biological activity in terms of either ROS production or resistance induction. This hypothesis is partially in opposition to the previous proposal that elicitins could activate two signal pathways (*8*). In that study it was proposed that first signal pathway was associated with early events, such as ROS production, and could be conditioned by a conformational change of the ω-loop induced by the sterol binding; and that a another pathway induced PR protein expression and hypersensitive response, and was dependent only on the overall structure of the elicitin and its charge distribution. The results presented here show that the observed conformational change of the ω-loop might not play so important a role. A more important role is probably played by small methionine and leucine residues in the ω-loop. Substitution of these with large phenylalanine and tryptophan residues probably alters the interaction of the elicitin with the binding site on the plasma membrane. In the previous study only a limited spectrum of transcripts was analysed, by northern blot analysis, and resistance was not evaluated, so the overall effect of the mutations was unknown. All this speculation could be supported by the fact that the L41F mutant was unable to stimulate the synthesis of ROS but triggered accumulation of some transcripts.

To conclude, these results generally agree with the hypothesis that the ability of elicitins to express PR proteins and to induce cell necroses and resistance is driven by the overall protein structure and charge distribution, with sterol binding playing only a minor role. However, only detailed characterization of cryptogein interaction with the high affinity binding site on the plasma membrane can fully explain the role of these factors in the biological activity of elicitins.

## *Literature*

1.  Scheel, D., and Nuernberger, T. (2004) Signal Transduction in Plant Defense Responses to Fungal Infection, in *Fungal Disease Resistance in Plants* (Punja, Z. K., Ed.), pp 1-30, The Haworth Press, Inc., Binghamton.
2.  Knogge, W. (1998) Fungal pathogenicity, *Current Opinion in Plant Biology 1*, 324-328.
3.  Benhamou, N., and Nicole, M. (1999) Cell biology of plant immunization against microbial infection: The potential of induced resistance in controlling plant diseases, *Plant Physiol. Biochem. 37*, 703-719.
4.  Vidhyasekaran, P. (2008) *Fungal Pathogenesis in Plants and Crops: Molecular Biology and Host Defense Mechanisms*, 2nd ed., Taylor & Francis Group, Boca Raton.
5.  Berger, S., Sinha, A. K., and Roitsch, T. (2007) Plant physiology meets phytopathology: plant primary metabolism and plant pathogen interactions, *Journal of Experimental Botany 58*, 4019-4026.
6.  Buchanan, B. B., Gruissem, W., and Jones, R. L. (2000) *Biochemistry & molecular biology of plants*, American Society of Plant Physiologists, Rockville.
7.  Dobeš, P., Kmuníček, J., Mikeš, V., and Damborský, J. (2004) Binding of Fatty Acids to β-Cryptogein: Quantitative Structure-Activity Relationships and Design of Selective Protein Mutants, *Journal of Chemical Information and Computer Sciences 44*, 2126-2132.
8.  Lochman, J., Kašparovský, T., Damborský, J., Osman, H., Marais, A., Chaloupková, R., Ponchet, M., Blein, J.-P., and Mikeš, V. (2005) Construction of Cryptogein Mutants, a Proteinaceous Elicitor from Phytophthora, with Altered Abilities To Induce a Defense Reaction in Tobacco Cells, *Biochemistry 44*, 6565-6572.
9.  Sanders, D., Brownlee, C., and Harper, J. F. (1999) Communicating with Calcium, *Plant Cell 11*, 691-706.
10. Lecourieux-Ouaked, F., Pugin, A., and Lebrun-Garcia, A. (2007) Phosphoproteins Involved in the Signal Transduction of Cryptogein, an Elicitor of Defense Reactions in Tobacco, *Molecular Plant-Microbe Interactions 13*, 821-829.
11. Sanders, D., Pelloux, J., Brownlee, C., and Harper, J. F. (2002) Calcium at the Crossroads of Signaling, *Plant Cell 14*, S401-417.
12. Wendehenne, D., Lamotte, O., Frachisse, J.-M., Barbier-Brygoo, H., and Pugin, A. (2002) Nitrate Efflux Is an Essential Component of the Cryptogein Signaling Pathway Leading to Defense Responses and Hypersensitive Cell Death in Tobacco, *Plant Cell 14*, 1937-1951.
13. Zhang, S., and Klessig, D. F. (2001) MAPK cascades in plant defense signaling, *Trends in Plant Science 6*, 520-527.
14. Lynch, D. V., and Dunn, T. M. (2004) An introduction to plant sphingolipids and a review of recent advances in understanding their metabolism and function, *New Phytologist 161*, 677-702.
15. Sakano, K., and Kwang, W. J. (2001) Metabolic regulation of pH in plant cells: Role of cytoplasmic pH in defense reaction and secondary metabolism, in *International Review of Cytology*, pp 1-44, Academic Press.
16. Auh, C. K., and Murphy, T. M. (1995) Plasma Membrane Redox Enzyme Is Involved in the Synthesis of $O_2-$ and $H_2O_2$ by Phytophthora Elicitor-Stimulated Rose Cells, *Plant Physiol. 107*, 1241-1247.
17. Sutherland, M. W. (1991) The generation of oxygen radicals during host plant responses to infection, *Physiological and Molecular Plant Pathology 39*, 79-93.
18. Mehdy, M. C. (1994) Active Oxygen Species in Plant Defense against Pathogens, *Plant Physiol. 105*, 467-472.
19. Scandalios, J. G. (1993) Oxygen Stress and Superoxide Dismutases, *Plant Physiol. 101*, 7-12.
20. Wojtaszek, P. (1997) Oxidative burst: an early plant response to pathogen infection, *Biochem. J. 322*, 681-692.
21. Lamotte, O., Gould, K., Lecourieux, D., Sequeira-Legrand, A., Lebrun-Garcia, A., Durner, J., Pugin, A., and Wendehenne, D. (2004) Analysis of Nitric Oxide Signaling Functions in Tobacco Cells Challenged by the Elicitor Cryptogein, *Plant Physiol. 135*, 516-529.
22. Bethke, P. C., Badger, M. R., and Jones, R. L. (2004) Apoplastic Synthesis of Nitric Oxide by Plant Tissues, *Plant Cell 16*, 332-341.
23. Klessig, D. F., Durner, J. r., Noad, R., Navarre, D. A., Wendehenne, D., Kumar, D., Zhou, J. M., Shah, J., Zhang, S., Kachroo, P., Trifa, Y., Pontier, D., Lam, E., and Silva, H. (2000) Nitric oxide and salicylic acid signaling in plant defense, *Proceedings of the National Academy of Sciences of the United States of America 97*, 8849-8855.
24. Raskin, I. (1992) Salicylate, A New Plant Hormone, *Plant Physiol. 99*, 799-803.
25. Delaney, T. P., Uknes, S., Vernooij, B., Friedrich, L., Weymann, K., Negrotto, D., Gaffney, T., Gut-Rella, M., Kessmann, H., Ward, E., and Ryals, J. (1994) A Central Role of Salicylic Acid in Plant Disease Resistance, *Science 266*, 1247-1250.
26. Durner, J., Shah, J., and Klessig, D. F. (1997) Salicylic acid and disease resistance in plants, *Trends in Plant Science 2*, 266-274.

27. Creelman, R. A., and Mullet, J. E. (2003) Biosynthesis and Action of Jasmonates in Plants, *Annual Review of Plant Physiology and Plant Molecular Biology 48*, 355-381.

28. Reinbothe, S., Mollenhauer, B., and Reinbothe, C. (1994) JIPs and RIPs: The Regulation of Plant Gene Expression by Jasmonates in Response to Environmental Cues and Pathogens, *Plant Cell 6*, 1197-1209.

29. Geraats, B. P. J., Bakker, P. A. H. M., Lawrence, C. B., Achuo, E. A., Höfte, M., and van Loon, L. C. (2007) Ethylene-Insensitive Tobacco Shows Differentially Altered Susceptibility to Different Pathogens, *Phytopathology 93*, 813-821.

30. Anderson, J. P., Badruzsaufari, E., Schenk, P. M., Manners, J. M., Desmond, O. J., Ehlert, C., Maclean, D. J., Ebert, P. R., and Kazan, K. (2004) Antagonistic Interaction between Abscisic Acid and Jasmonate-Ethylene Signaling Pathways Modulates Defense Gene Expression and Disease Resistance in Arabidopsis, *Plant Cell 16*, 3460-3479.

31. Loake, G., and Grant, M. (2007) Salicylic acid in plant defense--the players and protagonists, *Current Opinion in Plant Biology 10*, 466-472.

32. Spoel, S. H., Koornneef, A., Claessens, S. M. C., Korzelius, J. P., Van Pelt, J. A., Mueller, M. J., Buchala, A. J., Metraux, J.-P., Brown, R., Kazan, K., Van Loon, L. C., Dong, X., and Pieterse, C. M. J. (2003) NPR1 Modulates Cross-Talk between Salicylate- and Jasmonate-Dependent Defense Pathways through a Novel Function in the Cytosol, *Plant Cell 15*, 760-770.

33. Stuible, H.-P., and Kombrink, E. (2004) The Hypersensitive Response and Its Role in Disease Resistance, in *Fungal Disease Resistance in Plants* (Punja, Z. K., Ed.), pp 57-92, The Haworth Press, Inc., Binghamton.

34. Heath, M. C. (1998) Apoptosis, programmed cell death and the hypersensitive response, *European Journal of Plant Pathology 104*, 117-124.

35. Morel, J.-B., and Dangl, J. L. (1997) The hypersensitive response and the induction of cell death in plants, *Cell Death and Differentiation 4*, 671-683.

36. Richael, C., and Gilchrist, D. (1999) The hypersensitive response: A case of hold or fold?, *Physiological and Molecular Plant Pathology 55*, 5-12.

37. VanEtten, H. D., Mansfield, J. W., Bailey, J. A., and Farmer, E. E. (1994) Two Classes of Plant Antibiotics: Phytoalexins versus "Phytoanticipins", *Plant Cell 6*, 1191-1192.

38. Brindle, P. A., Kuhn, P. J., and Threlfall, D. R. (1983) Accumulation of phytoalexins in potato-cell suspension cultures, *Phytochemistry 22*, 2719-2721.

39. Jayaraj, J., Anand, A., and Muthukrishnan, S. (2004) Pathogenesis-Related Proteins and Their Roles in Resistance to Fungal Pathogens, in *Fungal Disease Resistance in Plants* (Punja, Z. K., Ed.), The Haworth Press, Inc., Binghamton.

40. van Loon, L. C. (1990) The nomenclature of pathogenesis-related proteins, *Physiological and Molecular Plant Pathology 37*, 229-230.

41. van Kan, J. A. L., Joosten, M. H. A. J., Wagemakers, C. A. M., Berg-Velthuis, G. C. M., and Wit, P. J. G. M. (1992) Differential accumulation of mRNAs encoding extracellular and intracellular PR proteins in tomato induced by virulent and avirulent races of Cladosporium fulvum, *Plant Molecular Biology 20*, 513-527.

42. Métrauxs, J.-P. (2001) Systemic Acquired Resistance And Salicylic Acid: Current State Of Knowledge, *European Journal of Plant Pathology 107*, 13-18.

43. Matsuoka, K., Matsumoto, S., Hattori, T., Machida, Y., and Nakamura, K. (1990) Vacuolar targeting and posttranslational processing of the precursor to the sweet potato tuberous root storage protein in heterologous plant cells, *Journal of Biological Chemistry 265*, 19750-19757.

44. Grenier, J., Potvin, C., Trudel, J., and Asselin, A. (1999) Some thaumatin-like proteins hydrolyse polymeric β-1,3-glucans, *The Plant Journal 19*, 473-480.

45. Yun, D.-J., Ibeas, J. I., Lee, H., Coca, M. A., Narasimhan, M. L., Uesono, Y., Hasegawa, P. M., Pardo, J. M., and Bressan, R. A. (1998) Osmotin, a Plant Antifungal Protein, Subverts Signal Transduction to Enhance Fungal Cell Susceptibility, *Molecular Cell 1*, 807-817.

46. Ride, J. P. (1983) Cell walls and other structural barriers in defense., in *Biochemical Plant Pathology* (Callow, J. A., Ed.), pp 215-236, Wiley-Interscience, New York.

47. Wei, Y., Zhang, Z., Andersen, C. H., Schmelzer, E., Gregersen, P. L., Collinge, D. B., Smedegaard-Petersen, V., and Thordal-Christensen, H. (1998) An epidermis/papilla-specific oxalate oxidase-like protein in the defense response of barley attacked by the powdery mildew fungus, *Plant Molecular Biology 36*, 101-112.

48. Zhang, Z., Collinge, D. B., and Thordal-Christensen, H. (1995) Germin-like oxalate oxidase, a H2O2-producing enzyme, accumulates in barley attacked by the powdery mildew fungus, *The Plant Journal 8*, 139-145.

49. Okushima, Y., Koizumi, N., Kusano, T., and Sano, H. (2000) Secreted proteins of tobacco cultured BY2 cells: identification of a new member of pathogenesis-related proteins, *Plant Molecular Biology 42*, 479-488.

50. Pliyev, B. K., and Gurvits, B. Y. (1999) Peptidyl-prolyl cis-trans isomerases: structure and functions, *Biochemistry (Mosc) 64*, 738-751.

51. Ye, X. Y., and Ng, T. B. (2001) Isolation of Unguilin, a Cyclophilin-Like Protein with Anti-Mitogenic, Antiviral, and Antifungal Activities, from Black-Eyed Pea, *Journal of Protein Chemistry 20*, 353-359.

52. Ye, X. Y., and Ng, T. B. (2000) Mungin, a Novel Cyclophilin-like Antifungal Protein from the Mung Bean, *Biochemical and Biophysical Research Communications 273*, 1111-1115.

53. Ye, X. Y., and Ng, T. B. (2002) Isolation of a new cyclophilin-like protein from chickpeas with mitogenic, antifungal and anti-HIV-1 reverse transcriptase activities, *Life Sciences 70*, 1129-1138.

54. Boissy, G., Fortelle, E. d. L., Kahn, R., Huet, J.-C., Bricogne, G., Pernollet, J.-C., and Brunie, S. (1996) Crystal structure of a fungal elicitor secreted by Phytophthora cryptogea, a member of a novel class of plant necrotic proteins, *Structure 4*, 1429-1439.

55. Gooley, P. R., Keniry, M. A., Dimitrov, R. A., Marsh, D. E., Keizer, D. W., Gayler, K. R., and Grant, B. R. (1998) The NMR solution structure and characterization of pH dependent chemical shifts of the β-elicitin, cryptogein, *Journal of Biomolecular NMR 12*, 523-534.

56. Blein, J.-P., Coutos-Thévenot, P., Marion, D., and Ponchet, M. (2002) From elicitins to lipid-transfer proteins: a new insight in cell signalling involved in plant defense mechanisms, *Trends in Plant Science 7*, 293-296.

57. Mikeš, V., Milat, M.-L., Ponchet, M., Panabieres, F., Ricci, P., and Blein, J.-P. (1998) Elicitins, Proteinaceous Elicitors of Plant Defense, Are a New Class of Sterol Carrier Proteins, *Biochemical and Biophysical Research Communications 245*, 133-139.

58. Vauthrin, S., Mikeš, V., Milat, M.-L., Ponchet, M., Maume, B., Osman, H., and Blein, J.-P. (1999) Elicitins trap and transfer sterols from micelles, liposomes and plant plasma membranes, *Biochimica et Biophysica Acta (BBA) - Biomembranes 1419*, 335-342.

59. Bourque, S., Binet, M.-N. l., Ponchet, M., Pugin, A., and Lebrun-Garcia, A. (1999) Characterization of the Cryptogein Binding Sites on Plant Plasma Membranes, *Journal of Biological Chemistry 274*, 34699-34705.

60. Viard, M. P., Martin, F., Pugin, A., Ricci, P., and Blein, J. P. (1994) Protein Phosphorylation Is Induced in Tobacco Cells by the Elicitor Cryptogein, *Plant Physiol. 104*, 1245-1249.

61. Kašparovský, T., Blein, J.-P., and Mikeš, V. (2004) Ergosterol elicits oxidative burst in tobacco cells via phospholipase A2 and protein kinase C signal pathway, *Plant Physiology and Biochemistry 42*, 429-435.

62. Binet, M.-N., Humbert, C., Lecourieux, D., Vantard, M., and Pugin, A. (2001) Disruption of Microtubular Cytoskeleton Induced by Cryptogein, an Elicitor of Hypersensitive Response in Tobacco Cells, *Plant Physiol. 125*, 564-572.

63. Osman, H., Vauthrin, S., Mikeš, V., Milat, M.-L., Panabieres, F., Marais, A., Brunie, S., Maume, B., Ponchet, M., and Blein, J.-P. (2001) Mediation of Elicitin Activity on Tobacco Is Assumed by Elicitin-Sterol Complexes, *Mol. Biol. Cell 12*, 2825-2834.

64. Mikeš, V., Milat, M.-L., Ponchet, M., Ricci, P., and Blein, J.-P. (1997) The fungal elicitor cryptogein is a sterol carrier protein, *FEBS Letters 416*, 190-192.

65. Stratagene QuickChange II XL Site-Directed Mutagenesis Kit. Instruction Manual.

66. Curran, B., and Bugeja, V. (2005) The biotechnological exploitation of heterologous protein production in fungi, in *Fungi: Biology and Applications* (Kavanagh, K., Ed.), pp 145-169, John Wiley & Sons, Ltd.

67. AmershamBiosciences. 2-D Electrophoresis using immobilized pH gradients. Principles and Methods.

68. Bio-Rad. 2-D Electrophoresis for Proteomics. A Methods and Product Manual.

69. Avdulov, N. A., Chochina, S. V., Igbavboa, U., Warden, C. S., Schroeder, F., and Wood, W. G. (1999) Lipid binding to sterol carrier protein-2 is inhibited by ethanol, *Biochimica et Biophysica Acta (BBA) - Molecular and Cell Biology of Lipids 1437*, 37-45.

70. Poinssot, B., Vandelle, E., Bentejac, M., Adrian, M., Levis, C., Brygoo, Y., Garin, J., Sicilia, F., Coutos-Thevenot, P., and Pugin, A. (2003) The endopolygalacturonase 1 from Botrytis cinerea activates grapevine defense reactions unrelated to its enzymatic activity, *Mol Plant Microbe Interact 16*, 553-564.

71. Ponchet, M., Panabieres, F., Milat, M. L., Mikes, V., Montillet, J. L., Suty, L., Triantaphylides, C., Tirilly, Y., and Blein, J. P. (1999) Are elicitins cryptograms in plant-oomycete communications?, *Cellular and Molecular Life Sciences 56*, 1020-1047.

72. Hugot, K., Aime, S., Conrod, S., Poupet, A., and Galiana, E. (1999) Developmental regulated mechanisms affect the ability of a fungal pathogen to infect and colonize tobacco leaves, *Plant Journal 20*, 163-170.

73. Galiana, E., Bonnet, P., Conrod, S., Keller, H., Panabieres, F., Ponchet, M., Poupet, A., and Ricci, P. (1997) RNase activity prevents the growth of a fungal pathogen in tobacco leaves and increases upon induction of systemic acquired resistance with elicitin, *Plant Physiology 115*, 1557-1567.

74. Slimestad, R., and Verheul, M. J. (2005) Seasonal Variations in the Level of Plant Constituents in Greenhouse Production of Cherry Tomatoes, *Journal of Agricultural and Food Chemistry 53*, 3114-3119.

75. Liu, B. Y., Lu, Y., Xin, Z. Y., and Zhang, Z. Y. (2009) Identification and antifungal assay of a wheat beta-1,3-glucanase, *Biotechnology Letters 31*, 1005-1010.

76. van Loon, L. C., Rep, M., and Pieterse, C. M. J. (2006) Significance of inducible defense-related proteins in infected plants. , *Annual Review of Phytopathology 44*, 135-162.

77. Grover, A., and Gowthaman, R. (2003) Strategies for development of fungus-resistant transgenic plants, *Current Science 84*, 330-340.

78. Ponstein, A. S., Bresvloemans, S. A., Selabuurlage, M. B., Vandenelzen, P. J. M., Melchers, L. S., and Cornelissen, B. J. C. (1994) A Novel Pathogen-Inducible and Wound-Inducible Tobacco (Nicotiana-Tabacum) Protein with Antifungal Activity, *Plant Physiology 104*, 109-118.

79. Caporale, C., Di Berardino, I., Leonardi, L., Bertini, L., Cascone, A., Buonocore, V., and Caruso, C. (2004) Wheat pathogenesis-related proteins of class 4 have ribonuclease activity, *Febs Letters 575*, 71-76.

80. Guevara-Morato, M., de Lacoba, M. G., Garcia-Luque, I., and Serra, M. T. (2010) Characterization of a pathogenesis-related protein 4 (PR-4) induced in Capsicum chinense L-3 plants with dual RNase and DNase activities, *Journal of Experimental Botany 61*, 3259-3271.

81. Rohini, V. K., and Rao, K. S. (2001) Transformation of peanut (Arachis hypogaea L.) with tobacco chitinase gene: variable response of transformants to leaf spot disease, *Plant Science 160*, 889-898.

82. Selabuurlage, M. B., Ponstein, A. S., Bresvloemans, S. A., Melchers, L. S., Vandenelzen, P. J. M., and Cornelissen, B. J. C. (1993) Only Specific Tobacco (Nicotiana-Tabacum) Chitinases and Beta-1,3-Glucanases Exhibit Antifungal Activity, *Plant Physiology 101*, 857-863.

83. Shinya, T., Hanai, K., Galis, I., Suzuki, K., Matsuoka, K., Matsuoka, H., and Saito, M. (2007) Characterization of NtChitIV, a class IV chitinase induced by beta-1,3-, 1,6-glucan elicitor from Alternaria alternata 102: Antagonistic effect of salicylic acid and methyl jasmonate on the induction of NtChitIV, *Biochemical and Biophysical Research Communications*, 311-317.

84. Melchers, L. S., Apothekerdegroot, M., Vanderknaap, J., Ponstein, A. S., Selabuurlage, M. B., Bol, J. F., Cornelissen, B. J. C., Vandenelzen, P. J. M., and Linthorst, H. J. M. (1994) A New Class of Tobacco Chitinases Homologous to Bacterial Exo-Chitinases Displays Antifungal Activity, *Plant Journal 5*, 469-480.

85. Hiraga, S., Ito, H., Sasaki, K., Yamakawa, H., Mitsuhara, I., Toshima, H., Matsui, H., Honma, M., and Ohashi, Y. (2000) Wound-induced expression of a tobacco peroxidase is not enhanced by ethephon and suppressed by methyl jasmonate and coronatine, *Plant and Cell Physiology 41*, 165-170.

86. Casaretto, J. A., and Corcuera, L. J. (1995) Plant proteinase inhibitors: a defensive response against insects, *Biol Res 28*, 239-249.

87. Wong, J. H., Ng, T. B., Cheung, R. C. F., Ye, X. J., Wang, H. X., Lam, S. K., Lin, P., Chan, Y. S., Fang, E. F., Ngai, P. H. K., Xia, L. X., Ye, X. Y., Jiang, Y., and Liu, F. (2010) Proteins with antifungal properties and other medicinal applications from plants and mushrooms, *Applied Microbiology and Biotechnology 87*, 1221-1235.

88. Manosalva, P. M., Davidson, R. M., Liu, B., Zhu, X. Y., Hulbert, S. H., Leung, H., and Leach, J. E. (2009) A Germin-Like Protein Gene Family Functions as a Complex Quantitative Trait Locus Conferring Broad-Spectrum Disease Resistance in Rice, *Plant Physiology 149*, 286-296.

89. Zimmermann, G., Baumlein, H., Mock, H. P., Himmelbach, A., and Schweizer, P. (2006) The multigene family encoding germin-like proteins of barley. Regulation and function in basal host resistance, *Plant Physiology 142*, 181-192.